J. Condensed Matter Nucl. Sci. 11 (2013) 15–58

Research Article

Central and Tensor Contributions to the Phonon-exchange Matrix Element for the $D_2/^4He$ Transition

Peter L. Hagelstein *

Research Laboratory of Electronics, Massachusetts Institute of Technology, Cambridge, MA 02139, USA

Irfan U. Chaudhary

Department of Computer Science and Engineering, University of Engineering and Technology. Lahore, Pakistan

Abstract

The biggest theoretical problem associated with excess heat in the Fleischmann–Pons experiment in our view has been the absence of energetic particles in amounts commensurate with the energy produced. In response we have pursued models in which the large nuclear energy quantum is fractionated into a great many lower energy quanta. To connect these idealized models to the physical system we need to evaluate the associated coupling matrix elements. Recently we have found a new coupling mechanism that arises when a lattice model is derived starting from a Dirac description of individual nucleons; this coupling mechanism can be considered a generalization of spin-orbit coupling and produces interactions between the center of mass dynamics and internal nuclear degrees of freedom. In this work we develop a simplified model for ^4He and molecular D_2 states with which we evaluate the phonon exchange matrix element for $D_2/^4He$ transitions based on the new interaction. We restrict our calculation to the central and tensor contributions of the Hamada–Johnston nucleon-nucleon potential, which are the strongest, and find coupling between ground state ^4He and triplet P and F molecular states. This interaction matrix element can be used in generalized lossy spin–boson models for the calculation of excess heat production in the Fleischmann–Pons experiment..
 ISSN 2227-3123

Keywords: $D_2/^4H$ phonon exchange matrix element, Excess heat, Fleischmann–Pons effect, Nuclear physics calculation, Phonon exchange, Selection rules

1. Introduction

We have for many years pursued the development of a theoretical model [1] to account for excess heat in the Fleischmann–Pons experiment [2–4]. From our perspective the biggest challenge for theory is the absence of energetic nuclear products in amounts commensurate with the energy produced [5]. Such an effect is unprecedented in nuclear physics, although there are effects which might be considered to be distant analogs in other areas of physics.

*E-mail: plh@mit.edu

 ISSN 2227-3123

We have studied new models in which efficient coherent energy exchange occurs between quantum systems with strongly mismatched characteristic energies [6–9]. These models are based on two-level systems coupled with an oscillator in the presence of strong loss effects. While these basic models have been under investigation now for more than a decade, it has been problematic connecting them with the physical system. In the model most relevant for excess heat production [10], there is a set of two-level systems that are weakly coupled to the oscillator; these stand in for a proposed $D_2/^4He$ transition. In addition there is a set of two-level systems that are strongly coupled to the oscillator; until recently it has not been clear what transitions in the physical system these might represent, since the coupling needed to be sufficiently strong that all reasonable electron–nuclear and electron–electron transitions could be ruled out (as too weak to fractionate the large MeV quantum).

The only transitions which could be sufficiently strong to make the model relevant to experiment are internal nuclear transitions, but until recently it was not obvious that there could be phonon exchange in such a transition. Earlier this year we developed a new fundamental lattice Hamiltonian that took as a starting point a Dirac model for electrons and nucleons, and we obtained an appropriate nonrelativistic limit that included mass effects as well as a new coupling between the center of mass an internal nuclear states [11]. In this model lattice vibrations are coupled to internal nuclear transitions as a result of relativistic effects, with the result that all compound nuclei have transitions that are candidates to fractionate a large quantum within the lossy spin–boson models.

In the Fleischmann–Pons experiments deuterium is loaded into palladium, so the most obvious candidates for the strongly coupled transitions are the deuterons and host Pd nuclei. In the two-laser experiments compressional optical phonon modes are implicated, suggesting that our focus should be on the deuterons since they move much more than the Pd nuclei when optical phonon modes are excited. We recently evaluated the deuteron coupling matrix element within the model [12], with the result that the coupling is very strong – much stronger than for any conventional (electron–nuclear or electron–electron) transition. Unfortunately, when we evaluated coherent energy exchange rates to compare with experiment we found that the coupling was still too weak. Recent work to be published shortly starts from a fundamental Hamiltonian based on quarks and electrons (instead of nucleons and electrons), which results in much larger coupling matrix elements. The model that results appears to be much more closely connected with experiment.

With a possible solution to the problem of the strongly-coupled transition in hand, our attention turns back to the $D_2/^4He$ system, where the coupling mechanism and associated phonon exchange have been of great interest. In nuclear physics the $d(d,\gamma)^4He$ reaction is known [13], and is weak since an electromagnetic interaction is involved [14] (the much stronger $d(d,n)^3He$ and d(d,p)t reactions are mediated by the strong force [15]). We had thought for many years that there might be a strong force mediated version of the $D_2/^4He$ transition with phonon exchange involved in the Fleischmann–Pons excess heat effect. The basic argument was that the difference between a local molecular D_2 and ^4He is sufficiently large that one would expect a very high probably for phonon exchange if the lattice is highly excited. A weakness of the argument is that the nuclear system on the fermi scale is very close to the vacuum system, so that one would expect the transition to be forbidden without some additional coupling.

If so, then we must return to the issue of how such a transition might occur consistent with physical law and the requirements of the lossy spin–boson models. There are a number of approaches that might be considered. We might contemplate electromagnetic coupling between the transition and the local electrons, which could be expected to lead to phonon exchange since the electronic orbitals respond to atomic motion associated with vibrations. Over the past year we have been wrestling with a similar approach in the case of nuclear excitation, where we explored many transitions mediated by electron–nuclear coupling. In general we found that the associated phonon exchange coupling matrix elements were small, and there is no reason not to think that the electron–nuclear coupling analog in the $D_2/^4He$ transition would not similarly be small. Given the recent computation of phonon exchange in the case of the $\mathbf{a} \cdot c\mathbf{P}$ coupling for the deuteron [12], which produced an interaction many orders of magnitude larger than possible for electron–nuclear coupling, it seems that we would do best by focusing on $\mathbf{a} \cdot c\mathbf{P}$ coupling for the $D_2/^4He$ transition.

The computation implied from this line of argument then is one in which we would evaluate the interaction matrix

element between a molecular D_2 state in the lattice, and the ground state ^{4}He state also in the lattice. In a relativistic model we could imagine evaluating the $\mathbf{a}\cdot c\mathbf{P}$ matrix element directly; in the nonrelativistic case we have available a reduction of the operator that we might use [11]. Unfortunately the nuclear four-body problem is much more complicated than the two-body problem was, and to carry out such a calculation even in the case of a simple nuclear potential model (such as the Hamada–Johnston potential [16]) involves considerable work.

An alternate approach in this case might instead be to carry out a much simpler calculation that assumes an approximate (not self-consistent) ^{1}S configuration for the ^{4}He, and use approximate molecular deuteron–deuteron fixed core wavefunctions based on reduced ^{3}S wavefunctions for individual deuterons. Within such an approach we might develop an approximate description that could be evaluated with a much more modest effort level. A more sophisticated calculation could be pursued in the future.

In what follows in this lengthy paper is a presentation of the associated calculation, with documentation of the associated details. In the nuclear physics literature in general the details of this kind of calculation do not get published. There are many reasons for this; for example, specific results for one potential in one formulation of a particular system do not extend to other systems, and as such they are not inherently interesting; and in the case of more complicated potential models the number of terms becomes very large, so that a documentation of the details would result in a very long paper. Here, we are dealing with one of the simpler potentials (and restricting our focus to only central and tensor contributions), so that we are not overwhelmed by a large number of contributions to the interaction. Also, this is the first calculation of the phonon exchange matrix element for the $D_2/^4$He transition, so we expect some interest in just how the coupling works and what is in the model. The relative absence of specific details about how one carries out such a calculation in the literature provided a hindrance to us in our calculations, so we are motivated here to present them in case others are interested in what we have done.

Some discussion of the calculation itself may be useful. The matrix element calculation involves spatial parts, spin parts, and isospin parts. Historically Racah algebra has been used to sort out the spin and isospin parts, and there is no reason that we should not make use of Racah algebra here. In practice, it seemed simpler to make use of Mathematica for a direct brute force evaluation of the spin and isospin parts of the matrix elements. A very large number of spatial integrals result from the reduction of the spin and isospin part of the problem, and we found that because of the high degree of symmetry of the spatial wavefunctions that they reduce down to only a few cases. As a result, by the end of the analysis we end up with relatively simple explicit formulas for the associated matrix element; for fixed center of mass momentum P (and no magnetic field coupling) we can write for the central potential contribution to the $l=1$ matrix element a result of the form

$$M_{\rm C}^{(S,M_{\rm S})} \;=\; (cP)\left[{\rm e}^{-G}\sqrt{\frac{R_0}{\langle R\rangle}\frac{(\Delta R)^2}{\langle(\Delta R)^2\rangle}}\right]_{l=1}\sum_{\kappa} A_{\rm C}^{\kappa}I_{\rm C}^{\kappa}+B_{\rm C}^{\kappa}J_{\rm C}^{\kappa}+C_{\rm C}^{\kappa}K_{\rm C}^{\kappa}+D_{\rm C}^{\kappa}L_{\rm C}^{\kappa},$$

which makes all parts of the problem explicit. The spin and isospin part of the problem now appears in the $A_{\rm C}$, $B_{\rm C}$, $C_{\rm C}$ and $D_{\rm C}$ expansion coefficients, which we tabulate. The spatial integrals show up as the $I_{\rm C}$, $J_{\rm C}$, $K_{\rm C}$ and $L_{\rm C}$ terms; since they are four-dimensional, there is no need to expand them in a series (as was typical in years past) because we can do the integrals numerically in this day and age with ease. We see that the Gamow factor associated with tunneling shows up explicitly as a prefactor; we also see prefactors associated with the relative molecular volume referenced to the molecule in vacuum. Finally, we have termed the interaction an $\mathbf{a}\cdot c\mathbf{P}$ interaction, so we see the cP part of the interaction explicitly in the prefactor (for z-directed motion), with the remaining terms combining to make up the associated a_z-matrix element.

2. Construction of the ^{4}He state

Since empirical nucleon-nucleon potentials depend explicitly on isospin, it is convenient to work with nuclear wavefunctions constructed using antisymmetric wavefunctions from space, spin and isospin pieces. In general we may write for such wavefunctions

$$\Psi \;=\; \sum_j c_j [R]_j [S]_j [T]_j , \tag{1}$$

where the $[R]_j$ are spatial terms, where the $[S]_j$ are spin-dependent terms, and where the $[T]_j$ are isospin-dependent terms [16,17].

In the case of the ^{4}He wavefunction, we can take advantage of the symmetric group construction. This allows us to identify the space, spin, and isospin terms directly with irreducible representations of the symmetric group, which we can write in terms of Yamanouchi symbols. Such a construction is also possible for the molecular D_2 wavefunction; however, the resulting expression is more complicated than what is possible from a simple factorization of the antisymmetrized wavefunction. Because of this, and also because our evaluation of the spin and isospin algebra will be done by brute force (so that we are not taking advantage of the nice properties of the Yamanouchi symbols), it will be convenient to work in terms of $[R]_j$, $[S]_j$, and $[T]_j$ functions.

2.1. Symmetric group construction of the helium ^{1}S state

We begin with a specification of the helium ^{1}S state wavefunction, which can be expanded as

$$\Psi_{^1\mathrm{S}} \;=\; [4321]_{RST} \;=\; [1111]_R [4321]_{ST} . \tag{2}$$

This formula may require some explanation in order to understand the associated construction. Nuclear wavefunctions in the isospin scheme are subject to the generalized Pauli principle that requires them to be antisymmetric upon exchange of any two nucleons. The first Yamanouchi symbol that appears ($[4321]_{RST}$) is one that says that the wavefunction made up of spatial (R), spin (S) and isospin (T) components must be fully antisymmetric upon substitution of any two nucleons $[4321]_{RST}$. On the right hand side is the decomposition into a fully symmetric spatial piece $[1111]_R$ and a fully antisymmetric spin and isospin piece $[4321]_{ST}$.

It is possible to decompose the fully antisymmetric spin and isospin piece into two different terms of mixed symmetry

$$[4321]_{ST} \;=\; \frac{1}{\sqrt{2}} \Big([2211]_S [2121]_T - [2121]_S [2211]_T \Big) . \tag{3}$$

This will allow us later on to separate the spin and isospin calculations. Overall, we may write the ^{4}He wavefunction as

$$\Psi_{^1\mathrm{S}} \;=\; \frac{1}{\sqrt{2}} [1111]_R \Big([2211]_S [2121]_T - [2121]_S [2211]_T \Big) . \tag{4}$$

2.2. Definition of $[R]$, $[S]$, and $[T]$ terms

The wavefunction described above is composed of two terms which we will denote as

$$\Psi_{^1\mathrm{S}} \;=\; \sum_{j=1}^{2} c_j [R]_j [S]_j [T]_j, \tag{5}$$

where

$$c_1 \;=\; \frac{1}{\sqrt{2}}, \qquad c_2 \;=\; -\frac{1}{\sqrt{2}}, \tag{6}$$

$$[R]_1 \;=\; [R]_2 \;=\; [1111]_R, \tag{7}$$

$$[S]_1 \;=\; [2211]_S, \qquad [T]_1 \;=\; [2121]_T, \tag{8}$$

$$[S]_2 \;=\; [2121]_S, \qquad [T]_2 \;=\; [2211]_T. \tag{9}$$

2.3. Spin pieces

We have available explicit representations of the spin functions for the singlet ($S = 0$) case (which for $M_S = 0$); these can be written as

$$[2211]_S \;=\; \frac{1}{\sqrt{12}}\Big[2\alpha(1)\alpha(2)\beta\ 3)\beta\ 4) + 2\beta\ 1)\beta\ 2)\alpha(3)\alpha(4) - \alpha(1)\beta\ 2)\alpha(3)\beta\ 4) - \beta\ 1)\alpha(2)\alpha(3)\beta\ 4) - \alpha(1)\beta\ 2)\beta\ 3)\alpha(4) - \beta\ 1)\alpha(2)\beta\ 3)\alpha(4)\Big], \tag{10}$$

$$[2121]_S \;=\; \frac{1}{2}\Big[\alpha(1)\beta\ 2)\alpha(3)\beta\ 4) - \beta\ 1)\alpha(2)\alpha(3)\beta\ 4) + \beta\ 1)\alpha(2)\beta\ 3)\alpha(4) - \alpha(1)\beta\ 2)\beta\ 3)\alpha(4)\Big]. \tag{11}$$

The notation here can be understood as defining whether a specific nucleon has an up or down spin

$$\alpha(j) \;=\; |\uparrow\rangle_j \;=\; \left|s = \frac{1}{2}, m_s = \frac{1}{2}\right\rangle, \tag{12}$$

$$\beta j) \;=\; |\downarrow\rangle_j \;=\; \left|s = \frac{1}{2}, m_s = -\frac{1}{2}\right\rangle. \tag{13}$$

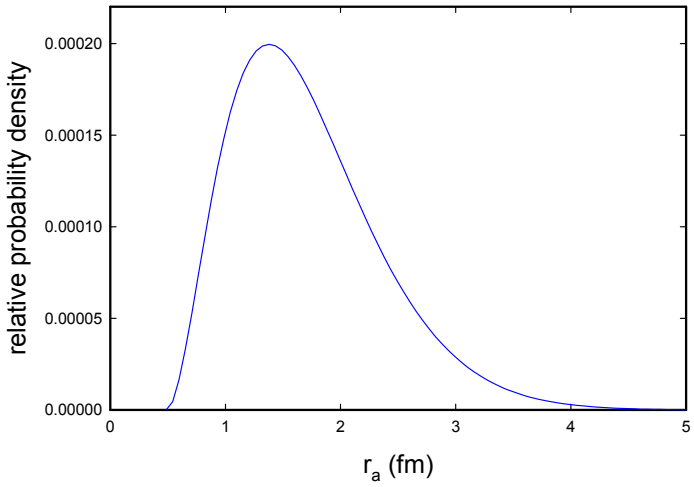

Figure 1. Relative probability distribution for nucleon–nucleon separation.

2.4. Isospin pieces

These basic formulas for the spin Yamanouchi symbols can be taken over to isospin directly (since the total isospin is zero) with the replacements

$$\alpha(j) \rightarrow \left| t = \frac{1}{2}, m_t = \frac{1}{2} \right\rangle, \tag{14}$$

$$\beta j) \rightarrow \left| t = \frac{1}{2}, m_t = -\frac{1}{2} \right\rangle. \tag{15}$$

2.5. Spatial part

The symmetry properties can be made clear using the notation

$$[R]_1 = [1111]_R = \Phi_S(\mathbf{r}_1, \mathbf{r}_2, \mathbf{r}_3, \mathbf{r}_4). \tag{16}$$

The requirement that Φ_S is fully symmetric can be written

$$\Phi_S(\mathbf{r}_1, \mathbf{r}_2, \mathbf{r}_3, \mathbf{r}_4) = \Phi_S(\mathbf{r}_2, \mathbf{r}_1, \mathbf{r}_3, \mathbf{r}_4) = \Phi_S(\mathbf{r}_3, \mathbf{r}_2, \mathbf{r}_1, \mathbf{r}_4) = \cdots, \tag{17}$$

where the $\cdots$ includes all permutations.

We adopt a symmetric wavefunction of the form

$$[R]_1 = N_S\, u(r_{21})u(r_{31})u(r_{41})u(r_{32})u(r_{42})u(r_{43}). \tag{18}$$

The form of the radial wavefunction $u(r)$ is

$$u(r) \;=\; (r - r_0)\mathrm{e}^{-\beta} \tag{19}$$

with

$$\beta \;=\; 0.928\ \mathrm{fm}^{-1}, \qquad r_0 \;=\; 0.485\ \mathrm{fm}, \qquad N_S \;=\; 0.7476\ \mathrm{fm}^{-21/2}. \tag{20}$$

These parameters were selected so that the mean square radius is matched to the equivalent radius for point nucleons from experiment

$$\sqrt{\langle |\mathbf{r} - \mathbf{R}|^2 \rangle} \;=\; 1.42\ \mathrm{fm}. \tag{21}$$

The normalization N_S is determined relative to a nine-dimensional integral expressed in molecular coordinates (to be discussed later on in this paper). The relative probability as a function of nucleon–nucleon separation for this model is shown in Fig. 1; it compares reasonably well to the relative probability for accurate wavefunctions (see [19]).

3. Construction of Molecular D_2 States

Our focus in this work will be on interaction matrix elements coupling to the molecular D_2 triplet states, since coupling to these states occur for the transition matrix element in connection with the central and tensor contributions to the Hamada–Johnston potential. However, more generally we are interested in coupling to the other states as well, and it is convenient to develop a systematic construction here for the other states as well.

3.1. Construction of anti-symmetrized wavefunctions

We would like to construct the nuclear wavefunctions for molecular D_2 using the generalized Pauli principle in the isospin scheme, since the empirical nucleon–nucleon potentials that we will be using are written explicitly in terms of isospin operators. The approach that we will use involves first constructing a suitable unsymmetrized wavefunction that has appropriate space, spin, and isospin components; and then make use of an antisymmetrization operator to produce a fully antisymmetric wavefunction. In general, we may write this as

$$\Psi \;=\; \mathcal{A}\Big\{[R][S][T]\Big\}, \tag{22}$$

where $[R]$, $[S]$, and $[T]$ denote space, spin, and isospin components, respectively.

3.2. Isospin component

The two nucleons that make up a deuteron in the ground state are in an isospin singlet state, so in all cases we may write

$$[T] \;=\; \frac{1}{2}\Big[\alpha(1)\beta\ 2) - \beta\ 1)\alpha(2)\Big]_T \Big[\alpha(3)\beta\ 4) - \beta\ 4)\alpha(3)\Big]_T, \tag{23}$$

where nucleons 1 and 2 are in one deuteron, and where nucleons 3 and 4 are in the other.

3.3. Spin components

Individual deuterons within the molecular are in triplet states, so we will make use of Clebsch–Gordan coefficients to construct the different spin states; we may write

$$|S_1 S_2 S M_S\rangle \;=\; \sum_{M_1+M_2=M_S} \langle S_1 S_2 M_1 M_2 | S_1 S_2 S M_S\rangle |S_1 S_2 M_1 M_2\rangle, \tag{24}$$

where $S_1 = S_2 = 1$. For the singlet case, we have

$$|S=0, M_S=0\rangle \;=\; \frac{1}{\sqrt{3}}\Big[|1,1\rangle_1|1,-1\rangle_2 - |1,0\rangle_1|1,0\rangle_2 + |1,-1\rangle_1|1,1\rangle_2\Big]. \tag{25}$$

For the three triplet cases, we may write

$$|S=1, M_S=-1\rangle \;=\; \frac{1}{\sqrt{2}}\Big[|1,0\rangle_1|1,-1\rangle_2 - |1,-1\rangle_1|1,0\rangle_2\Big], \tag{26}$$

$$|S=1, M_S=0\rangle \;=\; \frac{1}{\sqrt{2}}\Big[|1,1\rangle_1|1,-1\rangle_2 - |1,-1\rangle_1|1,1\rangle_2\Big], \tag{27}$$

$$|S=1, M_S=1\rangle \;=\; \frac{1}{\sqrt{2}}\Big[|1,1\rangle_1|1,0\rangle_2 - |1,0\rangle_1|1,1\rangle_2\Big]. \tag{28}$$

For the quintet states, we have

$$|S=2, M_S=-2\rangle \;=\; |1,-1\rangle_1|1,-1\rangle_2, \tag{29}$$

$$|S=2, M_S=-1\rangle \;=\; \frac{1}{\sqrt{2}}\Big[|1,0\rangle_1|1,-1\rangle_2 + |1,-1\rangle_1|1,0\rangle_2\Big], \tag{30}$$

$$|S=2, M_S=0\rangle \;=\; \frac{1}{\sqrt{6}}\Big[|1,1\rangle_1|1,-1\rangle_2 + 2|1,0\rangle_1|1,0\rangle_2 + |1,-1\rangle_1|1,1\rangle_2\Big], \tag{31}$$

$$|S=2, M_S=1\rangle \;=\; \frac{1}{\sqrt{2}}\Big[|1,1\rangle_1|1,0\rangle_2 + |1,0\rangle_1|1,1\rangle_2\Big], \tag{32}$$

$$|S=2, M_S=2\rangle \;=\; |1,1\rangle_1|1,1\rangle_2. \tag{33}$$

3.4. Spatial components

The associated spatial wavefunction should be of the form

$$[R] \;=\; \phi_d(r_{21})\phi_d(r_{43})R(r)Y_{lm}(\theta,\phi) \;=\; R(12;34). \tag{34}$$

We write for the molecular wavefunction the product $R(r)Y_{lm}(\theta,\phi)$ where r, θ, and ϕ are the spherical coordinates associated with the molecular relative coordinate $\mathbf{r}$ defined according to

$$\mathbf{r} \;=\; \frac{\mathbf{r}_3+\mathbf{r}_4}{2} - \frac{\mathbf{r}_1+\mathbf{r}_2}{2}. \tag{35}$$

For the spin triplet case l must be odd; for the singlet and quintet cases l must be even.

3.5. Antisymmetric molecular singlet state

We have used Mathematica to analyze the (unnormalized) antisymmetric singlet wavefunction, and we find that it simplifies to

$$\begin{aligned}
\mathcal{A}\Big\{[R][S][T]\Big\} \;=\;& R(12;34)\Big[(\alpha(1)\not\beta\ 2) - \not\beta\ 1)\alpha(2))(\alpha(3)\not\beta\ 4) - \not\beta\ 3)\alpha(4))\Big]_T \\
& \Big[2\alpha(1)\alpha(2)\not\beta\ 3)\not\beta\ 4) - \alpha(1)\not\beta\ 2)\alpha(3)\not\beta\ 4) - \alpha(1)\not\beta\ 2)\not\beta\ 3)\alpha(4) \\
& - \not\beta\ 1)\alpha(2)\alpha(3)\not\beta\ 4) - \not\beta\ 1)\alpha(2)\not\beta\ 3)\alpha(4) + 2\not\beta\ 1)\not\beta\ 2)\alpha(3)\alpha(4)\Big]_S \\
& - R(13;24)\Big[(\alpha(1)\not\beta\ 3) - \not\beta\ 1)\alpha(3))(\alpha(2)\not\beta\ 4) - \not\beta\ 2)\alpha(4))\Big]_T \\
& \Big[2\alpha(1)\not\beta\ 2)\alpha(3)\not\beta\ 4) - \alpha(1)\alpha(2)\not\beta\ 3)\not\beta\ 4) - \alpha(1)\not\beta\ 2)\not\beta\ 3)\alpha(4) \\
& - \not\beta\ 1)\not\beta\ 2)\alpha(3)\alpha(4) - \not\beta\ 1)\alpha(2)\alpha(3)\not\beta\ 4) + 2\not\beta\ 1)\alpha(2)\not\beta\ 3)\alpha(4)\Big]_S \\
& + R(14;23)\Big[(\alpha(1)\not\beta\ 4) - \not\beta\ 1)\alpha(4))(\alpha(2)\not\beta\ 3) - \not\beta\ 2)\alpha(3))\Big]_T \\
& \Big[2\alpha(1)\not\beta\ 2)\not\beta\ 3)\alpha(4) - \alpha(1)\not\beta\ 2)\alpha(3)\not\beta\ 4) - \alpha(1)\alpha(2)\not\beta\ 3)\not\beta\ 4) \\
& - \not\beta\ 1)\not\beta\ 2)\alpha(3)\alpha(4) - \not\beta\ 1)\alpha(2)\not\beta\ 3)\alpha(4) + 2\not\beta\ 1)\alpha(2)\alpha(3)\not\beta\ 4)\Big]_S .
\end{aligned} \tag{36}$$

We can write the resulting antisymmetrized wavefunction as a summation of the form

$$\Psi \;=\; \sum_{j=3}^{5} c_j [R]_j [S]_j [T]_j, \tag{37}$$

where we will work with $[R]_j$, $[S]_j$, and $[T]_j$ components that are individually normalized. For the isospin functions, we may write

$$[T]_3 \;=\; \frac{1}{2}\Big[(\alpha(1)\beta\ 2) - \beta\ 1)\alpha(2))(\alpha(3)\beta\ 4) - \beta\ 3)\alpha(4))\Big]_T, \tag{38}$$

$$[T]_4 \;=\; \frac{1}{2}\Big[(\alpha(1)\beta\ 3) - \beta\ 1)\alpha(3))(\alpha(2)\beta\ 4) - \beta\ 2)\alpha(4))\Big]_T, \tag{39}$$

$$[T]_5 \;=\; \frac{1}{2}\Big[(\alpha(1)\beta\ 4) - \beta\ 1)\alpha(4))(\alpha(2)\beta\ 3) - \beta\ 2)\alpha(3))\Big]_T. \tag{40}$$

For the spatial wavefunctions, we have

$$[R]_3 \;=\; R(12;34), \qquad [R]_4 \;=\; R(13;24), \qquad [R]_5 \;=\; R(14;23). \tag{41}$$

In the case of the expansion coefficients, we have

$$c_3 \;=\; c_5 \;=\; \frac{1}{\sqrt{3}}, \qquad c_4 \;=\; -\frac{1}{\sqrt{3}}. \tag{42}$$

The spin functions are different for the three cases; we may write

$$\begin{aligned}[S]_3 \;=\; \frac{1}{\sqrt{12}}\Big[&2\alpha(1)\alpha(2)\beta\ 3)\beta\ 4) - \alpha(1)\beta\ 2)\alpha(3)\beta\ 4) - \alpha(1)\beta\ 2)\beta\ 3)\alpha(4)\\ &- \beta\ 1)\alpha(2)\alpha(3)\beta\ 4) - \beta\ 1)\alpha(2)\beta\ 3)\alpha(4) + 2\beta\ 1)\beta\ 2)\alpha(3)\alpha(4)\Big]_S,\end{aligned} \tag{43}$$

$$\begin{aligned}[S]_4 \;=\; \frac{1}{\sqrt{12}}\Big[&2\alpha(1)\beta\ 2)\alpha(3)\beta\ 4) - \alpha(1)\alpha(2)\beta\ 3)\beta\ 4) - \alpha(1)\beta\ 2)\beta\ 3)\alpha(4)\\ &- \beta\ 1)\beta\ 2)\alpha(3)\alpha(4) - \beta\ 1)\alpha(2)\alpha(3)\beta\ 4) + 2\beta\ 1)\alpha(2)\beta\ 3)\alpha(4)\Big]_S,\end{aligned} \tag{44}$$

$$\begin{aligned}[S]_5 \;=\; \frac{1}{\sqrt{12}}\Big[&2\alpha(1)\beta\ 2)\beta\ 3)\alpha(4) - \alpha(1)\beta\ 2)\alpha(3)\beta\ 4) - \alpha(1)\alpha(2)\beta\ 3)\beta\ 4)\\ &- \beta\ 1)\beta\ 2)\alpha(3)\alpha(4) - \beta\ 1)\alpha(2)\beta\ 3)\alpha(4) + 2\beta\ 1)\alpha(2)\alpha(3)\beta\ 4)\Big]_S.\end{aligned} \tag{45}$$

3.6. Systematic construction of the molecular states

It is possible to develop a systematic construction for all of the molecular states using

$$\Psi \;=\; \frac{1}{\sqrt{3}}\Big([R]_3[S]_3[T]_3 - [R]_4[S]_4[T]_4 + [R]_5[S]_5[T]_5 \Big). \tag{46}$$

Based on the same c_j, $[R]_j$, and $[T]_j$ definitions given above for the singlet case. The spin functions $[S]_j$ are different, and we have tabulated unnormalized spin functions for all cases in Table 1. The notation we have used is as follows:

$$\begin{array}{llll}
s_1 = \alpha(1)\alpha(2)\alpha(3)\alpha(4), & s_2 = \alpha(1)\alpha(2)\alpha(3)\beta(4), & s_3 = \alpha(1)\alpha(2)\beta(3)\alpha(4), & s_4 = \alpha(1)\alpha(2)\beta(3)\beta(4), \\
s_5 = \alpha(1)\beta(2)\alpha(3)\alpha(4), & s_6 = \alpha(1)\beta(2)\alpha(3)\beta(4), & s_7 = \alpha(1)\beta(2)\beta(3)\alpha(4), & s_8 = \alpha(1)\beta(2)\beta(3)\beta(4), \\
s_9 = \beta(1)\alpha(2)\alpha(3)\alpha(4), & s_{10} = \beta(1)\alpha(2)\alpha(3)\beta(4), & s_{11} = \beta(1)\alpha(2)\beta(3)\alpha(4), & s_{12} = \beta(1)\alpha(2)\beta(3)\beta(4), \\
s_{13} = \beta(1)\beta(2)\alpha(3)\alpha(4), & s_{14} = \beta(1)\beta(2)\alpha(3)\beta(4), & s_{15} = \beta(1)\beta(2)\beta(3)\alpha(4), & s_{16} = \beta(1)\beta(2)\beta(3)\beta(4).
\end{array} \tag{47}$$

Certainly the various spin states are well known; however, the tabulation of the states in the form of Table 1 makes convenient their use systematically in Mathematica calculations.

Table 1. Tabulation of spin states $[S]^{(S,M_S)}$.

State	s_1	s_2	s_3	s_4	s_5	s_6	s_7	s_8	s_9	s_{10}	s_{11}	s_{12}	s_{13}	s_{14}	s_{15}	s_{16}
$[S]_3^{(0,0)}$	0	0	0	2	0	-1	-1	0	0	-1	-1	0	2	0	0	0
$[S]_4^{0,0}$	0	0	0	-1	0	2	-1	0	0	-1	2	0	-1	0	0	0
$[S]_5^{(0,0)}$	0	0	0	-1	0	-1	2	0	0	2	-1	0	-1	0	0	0
$[S]_3^{(1,-1)}$	0	0	0	0	0	0	0	1	0	0	0	1	0	-1	-1	0
$[S]_4^{(1,-1)}$	0	0	0	0	0	0	0	1	0	0	0	-1	0	1	-1	0
$[S]_5^{(1,-1)}$	0	0	0	0	0	0	0	1	0	0	0	-1	0	-1	1	0
$[S]_3^{(1,0)}$	0	0	0	1	0	0	0	0	0	0	0	0	-1	0	0	0
$[S]_4^{(1,0)}$	0	0	0	0	0	1	0	0	0	0	-1	0	0	0	0	0
$[S]_5^{(1,0)}$	0	0	0	0	0	0	1	0	0	-1	0	0	0	0	0	0
$[S]_3^{(1,1)}$	0	1	1	0	-1	0	0	0	-1	0	0	0	0	0	0	0
$[S]_4^{(1,1)}$	0	1	-1	0	1	0	0	0	-1	0	0	0	0	0	0	0
$[S]_5^{(1,1)}$	0	-1	1	0	1	0	0	0	-1	0	0	0	0	0	0	0
$[S]_3^{(2,-2)}$	0	0	0	0	0	0	0	0	0	0	0	0	0	0	0	1
$[S]_4^{(2,-2)}$	0	0	0	0	0	0	0	0	0	0	0	0	0	0	0	1
$[S]_5^{(2,-2)}$	0	0	0	0	0	0	0	0	0	0	0	0	0	0	0	1
$[S]_3^{(2,-1)}$	0	0	0	0	0	0	0	1	0	0	0	1	0	1	1	0
$[S]_4^{(2,-1)}$	0	0	0	0	0	0	0	1	0	0	0	1	0	1	1	0
$[S]_5^{(2,-1)}$	0	0	0	0	0	0	0	1	0	0	0	1	0	1	1	0
$[S]_3^{(2,0)}$	0	0	0	1	0	1	1	0	0	1	1	0	1	0	0	0
$[S]_4^{(2,0)}$	0	0	0	1	0	1	1	0	0	1	1	0	1	0	0	0
$[S]_5^{(2,0)}$	0	0	0	1	0	1	1	0	0	1	1	0	1	0	0	0
$[S]_3^{(2,1)}$	0	1	1	0	1	0	0	0	1	0	0	0	0	0	0	0
$[S]_4^{(2,1)}$	0	1	1	0	1	0	0	0	1	0	0	0	0	0	0	0
$[S]_5^{(2,1)}$	0	1	1	0	1	0	0	0	1	0	0	0	0	0	0	0
$[S]_3^{(2,2)}$	1	0	0	0	0	0	0	0	0	0	0	0	0	0	0	0
$[S]_4^{(2,2)}$	1	0	0	0	0	0	0	0	0	0	0	0	0	0	0	0
$[S]_5^{(2,2)}$	1	0	0	0	0	0	0	0	0	0	0	0	0	0	0	0

4. Molecular and Nuclear Deuteron Wavefunctions

We require a specification of the relative deuteron–deuteron molecular wavefunctions, and also the relative deuteron wavefunction, in order to evaluate the spatial integrals. For the molecular wavefunction we require estimates for the nuclear and Coulomb potentials, and then we must develop solutions to the radial Schrödinger equation. We will also need to worry about the wavefunction normalization which is made nontrivial due to the sizeable Gamow factors that appear in connection with tunneling through the Coulomb barrier. In the case of the nuclear wavefunction, we will need to develop a useful parameterization of the deuteron relative wavefunction.

4.1. Woods–Saxon potentials

Woods–Saxon potential parameters have been determined previously for deuteron–deuteron scattering. We may write for the different cases

$$V_{WS}^{(S,M_S)}(r) \;=\; \frac{V_S}{1+\mathrm{e}^{(r-r_S)/a_S}}, \tag{48}$$

where the fitting parameters from [20] are listed in Table 2.

4.2. Coulomb potential

The Coulomb potential between two deuterons within the approximation under discussion is given by

$$V_{\rm Coul}(r) \;=\; \left\langle R(12;34)\left|\frac{e^2}{r_{31}}\right|R(12;34)\right\rangle, \tag{49}$$

where the integrations are over the relative deuteron coordinates

$$\begin{aligned} V_{\rm Coul}(r) \;&=\; \left\langle \phi_d(r_{21})\phi_d(r_{43})\left|\frac{e^2}{r_{31}}\right|\phi_d(r_{21})\phi_d(r_{43})\right\rangle \\ &=\; \int \mathrm{d}^3\mathbf{r}_a \int \mathrm{d}^3\mathbf{r}_b\; \phi_d^2(r_a)\phi_d^b(r_b)\;\frac{e^2}{\sqrt{r^2+\left|\frac{\mathbf{r}_a-\mathbf{r}_b}{2}\right|^2}}. \end{aligned} \tag{50}$$

We have carried out a numerical evaluation of the Coulomb potential and fit the results in the form

Table 2. Woods–Saxon potential fitting parameters for deuteron–deuteron scattering.

S	l	V_S (MeV)	r_S (fm)	a_S (fm)
0	0	74	1.70	0.90
0	2	13.5	3.39	0.79
1	1	13.5	5.04	0.79
2	0	15.5	3.59	0.81

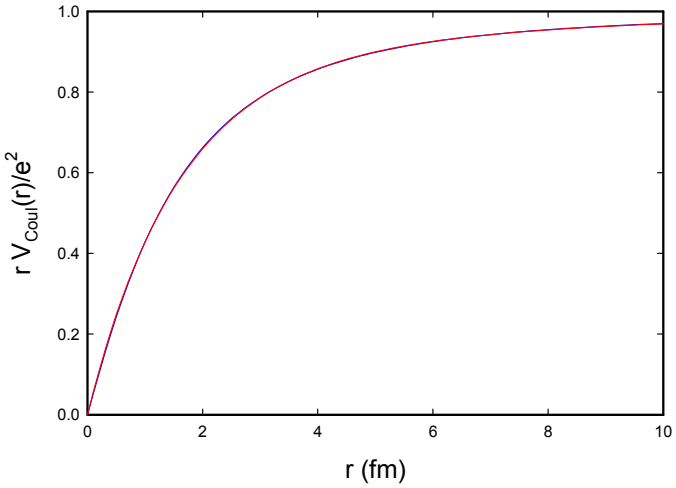

Figure 2. Scaled Coulomb potential between two deuterons; numerical calculation (*blue*); empirical fit (*red*). The two curves are seen to be very close together.

$$V_{\rm Coul}(r) \;=\; \frac{e^2}{r}\Big[1 - a{\rm e}^{-\kappa_1 r} - (1-a){\rm e}^{-\kappa_2 r}\Big] \tag{51}$$

with

$$a \;=\; 0.160807, \quad \kappa_1 \;=\; 0.170843\ {\rm fm}^{-1}, \quad \kappa_2 \;=\; 0.656377\ {\rm fm}^{-1}. \tag{52}$$

This fit is very good as illustrated in Fig. 2.

4.3. Molecular potential model

The deuteron–deuteron potential at short distances is made up of nuclear and Coulomb contributions as discussed above. At larger separation the deuterons see an attractive molecular potential. Since we are interested in the relative radial wavefunction, we will add the centripetal potential to make an effective potential. This allows us to write

$$V_{\rm eff}(r) \;=\; V_{WS}(r) + V_{\rm mol}(r) + \frac{\hbar^2 l(l+1)}{2\mu r^2}. \tag{53}$$

At larger separation we have made use of a molecular H_2 potential proposed by Frost and Musulin [21]

$$V_{\rm mol}(r) \;=\; \begin{cases} V_{\rm Coul}(r), & \text{small } r, \\ \dfrac{e^2}{a_0}{\rm e}^{-ar/a_0}\left(\dfrac{a_0}{r} - b\right), & \text{large } r \end{cases} \tag{54}$$

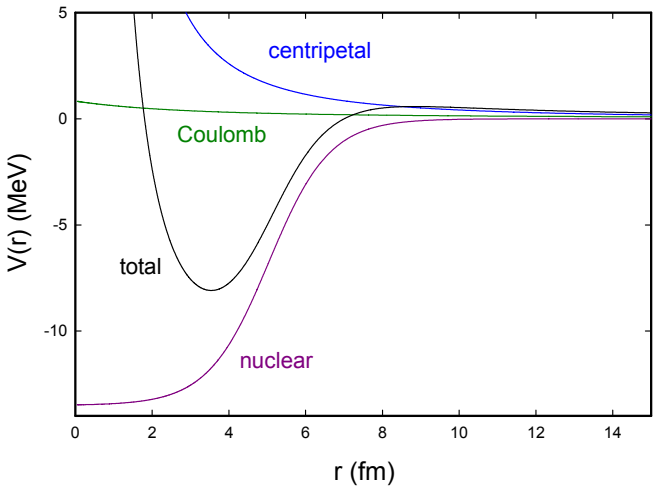

Figure 3. Deuteron–deuteron potential model, showing Wood–Saxon, Coulomb, and centripetal contributions.

with

$$a = 0.886, \qquad b = 1.315. \tag{55}$$

In Fig. 3, we show the different components along with the total deuteron–deuteron potential for the $l = 1$ channel in this model.

4.4. Schrödinger equation for the molecular radial wavefunction

The molecular radial wavefunction satisfies

$$E R(r) = -\frac{\hbar^2}{2\mu}\frac{1}{r^2}\frac{\mathrm{d}}{\mathrm{d}r}\left(r^2\frac{\mathrm{d}}{\mathrm{d}r}R(r)\right) + V_{\mathrm{eff}}(r)R(r), \tag{56}$$

where μ is the reduced mass

$$\mu = \frac{M_D}{2}. \tag{57}$$

4.5. Normalization of the molecular radial wavefunction

The normalization of the radial wavefunction is determined through

$$\int_0^\infty r^2 R^2(r)\mathrm{d}r = 1. \tag{58}$$

The normalization in this case is determined primarily by the wavefunction on the Angstrom scale; because of tunneling the wavefunction is very small on the fermi scale. Because screening effects are known to be important in metal deuterides, we would like to work with a scaled wavefunction near the origin where the tunneling effects have been removed.

We have decided to work with a scaled molecular radial wavefunction defined according to

$$R(r) \;=\; \frac{\mathrm{e}^{-G}}{\sqrt{R_0(\Delta R)^2}}\, F(r). \tag{59}$$

Here G is the Gamow factor

$$G \;=\; \int_{r_{\rm min}}^{r_{\rm max}} \sqrt{\frac{2\mu[V(r)-E]}{\hbar^2}}\mathrm{d}r. \tag{60}$$

The average separation and spread are given by

$$\langle r\rangle \;=\; R_0, \qquad (\Delta R)^2 \;=\; \langle (r-R_0)^2\rangle. \tag{61}$$

Defined in this way, our results will be roughly independent of the details of the particular molecular potential used. If screening is important, it will come in through the Gamow factor; if the molecular separation in the lattice is different, the associated volume effect is taken into account in the terms within the square root.

4.6. Model molecular radial wavefunctions

We have computed the molecular radial wavefunctions normalized as above, and fit them to

Table 3. Fitting parameters for the molecular D_2 wavefunctions; R_0 and ΔR in Angstroms; γ is in $\mathrm{fm}^{-1/2}$; A in fm^{-l}; b_1 and c_1 in fm^{-1}; b_2 and c_2 in fm^{-2}; and b_3 and c_3 in fm^{-3}.

Parameter	$S=0$ $l=0$	$S=2$ $l=0$	$S=1$ $l=1$	$S=0$ $l=2$	$S=2$ $l=2$	$S=1$ $l=3$
G	85.63	85.52	88.13	93.84	93.71	99.44
R_0	0.750	0.750	0.751	0.752	0.752	0.754
ΔR	0.0751	0.0751	0.0751	0.0752	0.0752	0.0753
γ	0.445321	0.447246	0.409238	0.367509	0.368575	0.327432
A	47.7563	28.6494	217.299	5.16205	5.12699	2.15563
b_1	-0.0574296	0.188016	-0.0856778	-0.225749	-0.227819	-0.218391
b_2	-0.148166	-0.0807753	0.00478186	0.0326325	0.0305096	0.0285951
b_3	-0.00449984	-0.00219149	1.16077×10^{-5}	3.72936×10^{-5}	3.35009×10^{-5}	2.234×10^{-5}
c_1	0.169052	0.412487	0.285851	-0.0557748	-0.053966	-0.0747202
c_2	0.204056	0.0257346	-0.141624	0.0238128	0.0177579	0.0215395
c_3	0.107872	0.0367975	0.0568277	0.00858995	0.00909683	0.0059147

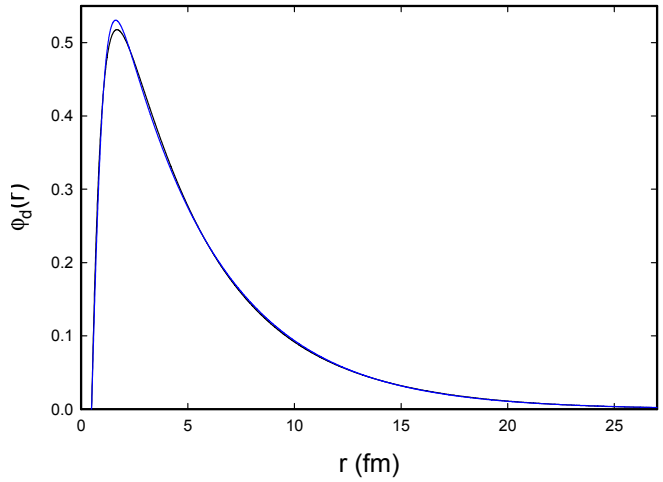

Figure 4. Triplet S channel deuteron wavefunction computed from the coupled-channel equations (*black*); and least squares fit (*blue*).

$$F(r) \;=\; Ar^l \frac{1 + b_1 r + b_2 r^2}{1 + c_1 r + c_2 r^2} \mathrm{e}^{-\gamma(\sqrt{r}+1)}. \tag{62}$$

where the 1 in the exponent is to be understood as $\sqrt{1\ \mathrm{fm}}$. Fitting parameters for the different radial molecular wavefunctions are given in Table 3.

4.7. Deuteron wavefunction

A reasonable approximation for a single deuteron wavefunction S channel is

$$\phi_d(r) \;=\; \begin{cases} 0 & \text{for } r < r_0, \\ N_d \dfrac{\tanh[\gamma(r - r_0)]\ \mathrm{e}^{-\beta}}{r} & \text{for } r_0 < r \end{cases} \tag{63}$$

From a least squares fit to a numerical solution of the Rarita–Schwinger equation based on the Hamada–Johnston potential, we obtain

$$\beta \;=\; 0.2159\ \mathrm{fm}^{-1}, \qquad \gamma \;=\; 1.460\ \mathrm{fm}^{-1}, \qquad N_d \;=\; 0.2132\ \mathrm{fm}^{-3/2}. \tag{64}$$

This function can provide a good fit to the model deuteron S channel wavefunction that we computed previously, as shown in Fig. 4.

5. Interaction

With a specification of the spin and isospin functions of the initial and final states, and with a clarification of the general form of the spatial wavefunctions, we now turn our attention to a specification of the interaction.

5.1. Relativistic $\mathbf{a} \cdot c\mathbf{P}$ interaction

In previous work we have derived the $\mathbf{a} \cdot c\mathbf{P}$ interaction starting with a many-nucleon Dirac model for the nuclei. In response to comments from a reviewer, we consider this approach under conditions where an external electromagnetic field is present. The relativistic nucleon Hamiltonian in the Dirac phenomenology in this case for a single nucleus can be written as

$$\hat{H} \;=\; \sum_j \boldsymbol{\alpha}_j \cdot c\left[\hat{\mathbf{p}}_j - \frac{e_j}{c}\hat{\mathbf{A}}(\mathbf{r}_j)\right] + \beta_j m_j c^2 + \sum_{j<k} V_{jk}(\mathbf{r}_k - \mathbf{r}_j), \tag{65}$$

where the nucleon–nucleon potential V_{jk} here is intended to include the strong force interaction as well as the electromagnetic interactions between nucleons within the nucleus; and where $\hat{\mathbf{A}}$ describes the external field.

Since the nuclear center of mass momentum is small for the problems of interest to us, we adopt nonrelativistic center of mass and relative coordinates

$$M\mathbf{R} \;=\; \sum_j m_j \mathbf{r}_j, \qquad \boldsymbol{\xi}_j \;=\; \mathbf{r}_j - \mathbf{R}, \tag{66}$$

$$\mathbf{P} \;=\; \sum_j \mathbf{p}_j, \qquad \boldsymbol{\pi}_j \;=\; \mathbf{p}_j - \frac{m_j}{M}\mathbf{P}. \tag{67}$$

Due to the close connection between the momentum and vector potential in the many-nucleon Dirac model, it may be best to adopt an analogous separation in the external field based on the total (charge-weighted) external field

$$\sum_j e_j \hat{\mathbf{A}}(\mathbf{r}_j) \;\rightarrow\; Ze\hat{\mathbf{A}}. \tag{68}$$

This allows us to achieve a separation between center of mass and relative contributions for the Hamiltonian

$$\begin{aligned}\hat{H} \;=\; & \sum_j \frac{m_j}{M}\boldsymbol{\alpha}_j \cdot \left(c\hat{\mathbf{P}} - Ze\hat{\mathbf{A}}\right) \\ & + \sum_j \boldsymbol{\alpha}_j \cdot \left(c\hat{\boldsymbol{\pi}}_j - e_j\hat{A}(\mathbf{r}_j) + \frac{m_j}{M}Ze\hat{\mathbf{A}}\right) + \sum_j \beta_j m_j c^2 + \sum_{j<k} V_{jk}(\boldsymbol{\xi}_k - \boldsymbol{\xi}_j).\end{aligned} \tag{69}$$

The first term includes center of mass interactions, and the remaining can be understood as describing relative interactions. In light of this the relativistic $\mathbf{a} \cdot c\mathbf{P}$ interaction should be

$$\hat{H}_{\rm int} \;=\; \sum_j \frac{m_j}{M}\boldsymbol{\alpha}_j \cdot \left(c\hat{\mathbf{P}} - Ze\hat{\mathbf{A}}\right) \tag{70}$$

instead of what we have used in earlier work where the contribution of the external field has not been included. We are indebted to the reviewer for pointing this out.

Some further discussion is probably helpful in thinking about the model that results. It does not come as a surprise that photon absorption and emission can be included in this kind of formulation (Eq. (69)), and in the separation that we have adopted we can see both center of mass and relative contributions explicitly. Since we are most interested in the center of mass interaction, it becomes important to understand what new physics is now included in the new interaction Hamiltonian of Eq. (70). If we adopt a Coulomb gauge point of view (which is predominant in atomic, molecular and condensed matter physics), then we would associate the new term with magnetic interactions (since Coulomb interactions are not included in the vector potential operator). This is interesting, since it tells us that there is a magnetic analog to the vibrational coupling that we have been focusing on, that we had not considered previously.

In what follows we will continue the analysis as if magnetic field effects can be neglected (working with **P** alone), and then revisit the issue in the conclusions.

5.2. Nonrelativistic $\mathbf{a}\cdot c\mathbf{P}$ Hamiltonian

For the nuclear calculation we adopt the equal mass part of the nonrelativistic expansion [11], which can be written as

$$\hat{H}_{\rm int} = \frac{1}{(2Mc^2)}\frac{1}{(2m_{av}c^2)} \sum_i \left\{ (\boldsymbol{\sigma}_i\cdot c\hat{\mathbf{P}})\left[\sum_{j<k}\hat{V}_{jk}\right](\boldsymbol{\sigma}_i\cdot c\hat{\boldsymbol{\pi}}_i) + (\boldsymbol{\sigma}_i\cdot c\hat{\boldsymbol{\pi}}_i)\left[\sum_{j<k}\hat{V}_{jk}\right](\boldsymbol{\sigma}_i\cdot c\hat{\mathbf{P}})\right\}, \tag{71}$$

where the $\hat{\boldsymbol{\pi}}_j$ operators are nucleon operators without the center of mass contribution.

$$\hat{\boldsymbol{\pi}}_j = \hat{\mathbf{p}}_j - \frac{\hat{\mathbf{P}}}{4}. \tag{72}$$

Note that in general this interaction involves three nucleons.

5.3. Two-body interaction

It appears that it is possible to simplify the interaction some. From an inspection of the interaction Hamiltonian, one sees that there are indices for three nucleons. When the index i matches j or k, we may isolate the contribution as

$$\hat{H}_{\rm int}^{2\,\rm body} = \frac{1}{(2Mc^2)}\frac{1}{(2m_{av}c^2)}\sum_{j<k}\Big\{(\boldsymbol{\sigma}_j\cdot c\hat{\mathbf{P}})\hat{V}_{jk}(\boldsymbol{\sigma}_j\cdot c\hat{\boldsymbol{\pi}}_j) + (\boldsymbol{\sigma}_j\cdot c\hat{\boldsymbol{\pi}}_j)\hat{V}_{jk}(\boldsymbol{\sigma}_j\cdot c\hat{\mathbf{P}})$$

$$+(\boldsymbol{\sigma}_k\cdot c\hat{\mathbf{P}})\hat{V}_{jk}(\boldsymbol{\sigma}_k\cdot c\hat{\boldsymbol{\pi}}_k) + (\boldsymbol{\sigma}_k\cdot c\hat{\boldsymbol{\pi}}_k)\hat{V}_{jk}(\boldsymbol{\sigma}_k\cdot c\hat{\mathbf{P}})\Big\}. \tag{73}$$

5.4. Three-body interaction

If the indices are all different then it seems that the associated operators will commute. In this case we may write

$$\hat{H}_{\rm int}^{\rm 3\,body} = \frac{1}{(2Mc^2)}\frac{1}{(2m_{\rm av}c^2)} \sum_i \sum_{j<k, j\neq i, k\neq i} \left\{ (\boldsymbol{\sigma}_i \cdot c\hat{\mathbf{P}}) \hat{V}_{jk} (\boldsymbol{\sigma}_i \cdot c\hat{\boldsymbol{\pi}}_i) + (\boldsymbol{\sigma}_i \cdot c\hat{\boldsymbol{\pi}}_i) \hat{V}_{jk} (\boldsymbol{\sigma}_i \cdot c\hat{\mathbf{P}}) \right\}. \tag{74}$$

In general we expect the operators associated with i to commute with $\hat{V}_{jk}$, which allows us to write

$$\begin{aligned} \hat{H}_{\rm int}^{\rm 3\,body} &= \frac{1}{(2Mc^2)}\frac{1}{(2m_{\rm av}c^2)} \sum_i \sum_{j<l, j\neq i, k\neq i} \hat{V}_{jk} \left[(\boldsymbol{\sigma}_i \cdot c\hat{\mathbf{P}})(\boldsymbol{\sigma}_i \cdot c\hat{\boldsymbol{\pi}}_i) + (\boldsymbol{\sigma}_i \cdot c\hat{\boldsymbol{\pi}}_i)(\boldsymbol{\sigma}_i \cdot c\hat{\mathbf{P}}) \right] \\ &= \frac{1}{(2m_{\rm av}c^2)} \sum_i \frac{\hat{\mathbf{P}} \cdot \hat{\boldsymbol{\pi}}_i}{M} \left[\sum_{j<k, j\neq i, k\neq i} \hat{V}_{jk} \right]. \end{aligned} \tag{75}$$

The three-body interaction vanishes in this case because

$$\sum_i \frac{\hat{\mathbf{P}} \cdot \hat{\boldsymbol{\pi}}_i}{M} = \frac{\hat{\mathbf{P}}}{M} \cdot \sum_i \hat{\boldsymbol{\pi}}_i = 0 \tag{76}$$

since the relative momentum operators sum to zero [11].

5.5. Hamada–Johnston potential

Because the nuclear potential models are very complicated, we have chosen to work with one of the early models that is relatively simple in form. The Hamada–Johnston potential can be written as [15]

$$\hat{V} = V_C + V_T \hat{S}_{12} + V_{LS} (\hat{\mathbf{L}} \cdot \hat{\mathbf{S}}) + V_{LL} \hat{L}_{12}. \tag{77}$$

It will be convenient to rewrite it in the form

$$\hat{V} = (\boldsymbol{\sigma}_1 \cdot \boldsymbol{\sigma}_2)(\boldsymbol{\tau}_1 \cdot \boldsymbol{\tau}_2) v_C(r) + (\boldsymbol{\tau}_1 \cdot \boldsymbol{\tau}_2) \hat{S}_{12} v_T(r) + \left(\frac{\hat{\mathbf{L}} \cdot \hat{\mathbf{S}}}{\hbar^2} \right) v_{LS}(r) + \left(\frac{\hat{L}_{12}}{\hbar^2} \right) v_{LL}(r), \tag{78}$$

where the different terms are described in the Appendix.

6. Reduction of Spin and Isospin for the Central Potential

We can write for the central potential contribution to the interaction matrix element

$$\hat{H}_C = \frac{1}{(2Mc^2)}\frac{1}{(2m_{\rm av}c^2)}\sum_{j<k}\Bigg\{ \Psi[^4\mathrm{He}]\Big|(\boldsymbol{\sigma}_j\cdot c\hat{\mathbf{P}})(\boldsymbol{\sigma}_j\cdot\boldsymbol{\sigma}_k)(\boldsymbol{\tau}_j\cdot\boldsymbol{\tau}_k)\hat{v}_C(r_{jk})(\boldsymbol{\sigma}_j\cdot c\hat{\boldsymbol{\pi}}_j)\Big|\Psi[\mathrm{D}_2]\Big\rangle$$
$$+\Big\langle\Psi[^4\mathrm{He}]\Big|(\boldsymbol{\sigma}_j\cdot c\hat{\boldsymbol{\pi}}_j)(\boldsymbol{\sigma}_j\cdot\boldsymbol{\sigma}_k)(\boldsymbol{\tau}_j\cdot\boldsymbol{\tau}_k)\hat{v}_C(r_{jk})(\boldsymbol{\sigma}_j\cdot c\hat{\mathbf{P}})\Big|\Psi[\mathrm{D}_2]\Big\rangle$$
$$+\Big\langle\Psi[^4\mathrm{He}]\Big|(\boldsymbol{\sigma}_k\cdot c\hat{\mathbf{P}})(\boldsymbol{\sigma}_j\cdot\boldsymbol{\sigma}_k)(\boldsymbol{\tau}_j\cdot\boldsymbol{\tau}_k)\hat{v}_C(r_{jk})(\boldsymbol{\sigma}_k\cdot c\hat{\boldsymbol{\pi}}_k)\Big|\Psi[\mathrm{D}_2]\Big\rangle$$
$$+\Big\langle\Psi[^4\mathrm{He}]\Big|(\boldsymbol{\sigma}_k\cdot c\hat{\boldsymbol{\pi}}_k)(\boldsymbol{\sigma}_j\cdot\boldsymbol{\sigma}_k)(\boldsymbol{\tau}_j\cdot\boldsymbol{\tau}_k)\hat{v}_C(r_{jk})(\boldsymbol{\sigma}_k\cdot c\hat{\mathbf{P}})\Big|\Psi[\mathrm{D}_2]\Big\rangle\Bigg\}. \tag{79}$$

Our interest ultimately is in the interaction as a lattice operator based on the center of mass operator $\hat{\mathbf{P}}$; however, for the specific calculations that we need to carry out to evaluate the nuclear part of the interaction the answers will be the same if we replace the operator $\hat{\mathbf{P}}$ with a constant momentum $\mathbf{P}$. Then, in order to simplify things, we take the center of mass momentum $\mathbf{P}$ to be z-directed

$$\mathbf{P} = P\hat{\mathbf{i}}_z \tag{80}$$

This allows us to write

$$M_C = \frac{P}{2M}\frac{1}{(2m_{\rm av}c^2)}\sum_{j<k}\Bigg\{ \Psi[^4\mathrm{He}]\Big|(\boldsymbol{\sigma}_j\cdot\hat{\mathbf{i}}_z)(\boldsymbol{\sigma}_j\cdot\boldsymbol{\sigma}_k)(\boldsymbol{\tau}_j\cdot\boldsymbol{\tau}_k)\hat{v}_C(r_{jk})(\boldsymbol{\sigma}_j\cdot\hat{\boldsymbol{\pi}}_j)\Big|\Psi[\mathrm{D}_2]\Big\rangle$$
$$+\Big\langle\Psi[^4\mathrm{He}]\Big|(\boldsymbol{\sigma}_j\cdot\hat{\boldsymbol{\pi}}_j)(\boldsymbol{\sigma}_j\cdot\boldsymbol{\sigma}_k)(\boldsymbol{\tau}_j\cdot\boldsymbol{\tau}_k)\hat{v}_C(r_{jk})(\boldsymbol{\sigma}_j\cdot\hat{\mathbf{i}}_z)\Big|\Psi[\mathrm{D}_2]\Big\rangle$$
$$+\Big\langle\Psi[^4\mathrm{He}]\Big|(\boldsymbol{\sigma}_k\cdot\hat{\mathbf{i}}_z)(\boldsymbol{\sigma}_j\cdot\boldsymbol{\sigma}_k)(\boldsymbol{\tau}_j\cdot\boldsymbol{\tau}_k)\hat{v}_C(r_{jk})(\boldsymbol{\sigma}_k\cdot\hat{\boldsymbol{\pi}}_k)\Big|\Psi[\mathrm{D}_2]\Big\rangle$$
$$+\Big\langle\Psi[^4\mathrm{He}]\Big|(\boldsymbol{\sigma}_k\cdot\hat{\boldsymbol{\pi}}_k)(\boldsymbol{\sigma}_j\cdot\boldsymbol{\sigma}_k)(\boldsymbol{\tau}_j\cdot\boldsymbol{\tau}_k)\hat{v}_C(r_{jk})(\boldsymbol{\sigma}_k\cdot\hat{\mathbf{i}}_z)\Big|\Psi[\mathrm{D}_2]\Big\rangle\Bigg\}. \tag{81}$$

6.1. Evaluation based on product formula

The computation of the interaction matrix elements involves spin, isospin, angular momentum and spatial matrix elements which at the outset are mixed together. Since we are using nuclear wavefunctions that are composed of simple products of space, spin and isospin we can take advantage of the factorization of the individual terms in the Hamiltonian. Since individual interactions factor, we may evaluate the contributions to the matrix element using the product formula

$$\langle\Psi_{^1\mathrm{S}}|\hat{O}_R\hat{O}_S\hat{O}_T|\Psi_{D_2}\rangle = \sum_{j=1}^{2}\sum_{k=3}^{5}c_jc_k\langle[R]_j|\hat{O}_R|[R]_k\rangle\langle[S]_j|\hat{O}_S|[S]_k\rangle\langle[T]_j|\hat{O}_T|[T]_k\rangle. \tag{82}$$

Specific computations that follow have been carried out using Mathematica to evaluate the spin and isospin matrix elements.

6.2. Central potential matrix element for singlet states

We can express the results of the Mathematica calculations for the molecular singlet state in the form

$$M_C^{(0,0)} = \frac{P}{2M}\frac{1}{(2m_{av}c^2)}\sum_{j<k}\sum_{\kappa}\sum_{\iota}\Bigg\{ a_C^{\kappa}(jk;\iota)\left\langle [R]_1\left|v_C^{\kappa}(r_{jk})(\hat{\mathbf{i}}_z\cdot\hat{\boldsymbol{\pi}}_j)\right|[R]_\iota\right\rangle + b_C^{\kappa}(jk;\iota)\left\langle [R]_1\left|\hat{v}_C(r_{jk})(\hat{\mathbf{i}}_z\cdot\hat{\boldsymbol{\pi}}_k)\right|[R]_\iota\right\rangle + c_C^{\kappa}(jk;\iota)\left\langle [R]_1\left|(\hat{\mathbf{i}}_z\cdot\hat{\boldsymbol{\pi}}_j)v_C^{\kappa}(r_{jk})\right|[R]_\iota\right\rangle + d_C^{\kappa}(jk;\iota)\left\langle [R]_1\left|(\hat{\mathbf{i}}_z\cdot\hat{\boldsymbol{\pi}}_k)\hat{v}_C(r_{jk})\right|[R]_\iota\right\rangle\Bigg\}. \tag{83}$$

A tabulation of explicit values for expansion coefficients in a different form will be presented for contributions that are not zero due to selection rules later on.

6.3. Central potential matrix element for the triplet states

For the triplet case, when $M_S = \pm 1$ we obtain

$$M_C^{(1,\pm1)} = \frac{P}{2M}\frac{1}{(2m_{\rm av}c^2)}\sum_{j<k}\sum_{\kappa}\sum_{\iota}\Bigg\{$$

$$a_C^{\kappa}(jk;\iota)\left\langle [R]_1\left|v_C^{\kappa}(r_{jk})\left[(\hat{\mathbf{i}}_x\pm\hat{\mathbf{i}}_y)\cdot\hat{\boldsymbol{\pi}}_j\right]\right|[R]_\iota\right\rangle + b_C^{\kappa}(jk;\iota)\left\langle [R]_1\left|\hat{v}_C(r_{jk})\left[(\hat{\mathbf{i}}_x\pm\hat{\mathbf{i}}_y)\cdot\hat{\boldsymbol{\pi}}_k\right]\right|[R]_\iota\right\rangle$$

$$+c_C^{\kappa}(jk;\iota)\left\langle [R]_1\left|\left[(\hat{\mathbf{i}}_x\pm\hat{\mathbf{i}}_y)\cdot\hat{\boldsymbol{\pi}}_j\right]v_C^{\kappa}(r_{jk})\right|[R]_\iota\right\rangle + d_C^{\kappa}(jk;\iota)\left\langle [R]_1\left|\left[(\hat{\mathbf{i}}_x\pm\hat{\mathbf{i}}_y)\cdot\hat{\boldsymbol{\pi}}_k\right]\hat{v}_C(r_{jk})\right|[R]_\iota\right\rangle\Bigg\}. \tag{84}$$

The coefficients for both cases $M_S = \pm 1$ are the same. When $M_S = 0$ there is no contribution

$$M_C^{(1,0)} = 0. \tag{85}$$

6.4. Central potential matrix element for the quintet states

Central potential contributions to the interaction matrix element are found for quintet states with $M_S = 0, \pm 1$. For the $M_S = 0$ case we may write

$$M_C^{(2,0)} = \frac{P}{2M}\frac{1}{(2m_{\rm av}c^2)}\sum_{j<k}\sum_{\kappa}\sum_{\iota}\Bigg\{ a_C^{\kappa}(jk;\iota)\left\langle [R]_1\left|v_C^{\kappa}(r_{jk})(\hat{\mathbf{i}}_z\cdot\hat{\boldsymbol{\pi}}_j)\right|[R]_\iota\right\rangle + b_C^{\kappa}(jk;\iota)\left\langle [R]_1\left|\hat{v}_C(r_{jk})(\hat{\mathbf{i}}_z\cdot\hat{\boldsymbol{\pi}}_k)\right|[R]_\iota\right\rangle + c_C^{\kappa}(jk;\iota)\left\langle [R]_1\left|(\hat{\mathbf{i}}_z\cdot\hat{\boldsymbol{\pi}}_j)v_C^{\kappa}(r_{jk})\right|[R]_\iota\right\rangle + d_C^{\kappa}(jk;\iota)\left\langle [R]_1\left|(\hat{\mathbf{i}}_z\cdot\hat{\boldsymbol{\pi}}_k)\hat{v}_C(r_{jk})\right|[R]_\iota\right\rangle\Bigg\}. \tag{86}$$

In the case of the quintet states with $M_S = \pm 1$, we may write

$$M_C^{(1,\pm 1)} = \frac{P}{2M}\frac{1}{(2m_{\rm av}c^2)}\sum_{j<k}\sum_{\kappa}\sum_{\iota}\Bigg\{$$

$$a_C^\kappa(jk;\iota)\Big\langle [R]_1\Big|v_C^\kappa(r_{jk})\Big[(\hat{\mathbf{i}}_x \pm i\hat{\mathbf{i}}_y)\cdot\hat{\boldsymbol{\pi}}_j\Big]\Big|[R]_\iota\Big\rangle + b_C^\kappa(jk;\iota)\Big\langle [R]_1\Big|\hat{v}_C(r_{jk})\Big[(\hat{\mathbf{i}}_x \pm i\hat{\mathbf{i}}_y)\cdot\hat{\boldsymbol{\pi}}_k\Big]\Big|[R]_\iota\Big\rangle$$

$$+c_C^\kappa(jk;\iota)\Big\langle [R]_1\Big|\Big[(\hat{\mathbf{i}}_x \pm i\hat{\mathbf{i}}_y)\cdot\hat{\boldsymbol{\pi}}_j\Big]v_C^\kappa(r_{jk})\Big|[R]_\iota\Big\rangle + d_C^\kappa(jk;\iota)\Big\langle [R]_1\Big|\Big[(\hat{\mathbf{i}}_x \pm i\hat{\mathbf{i}}_y)\cdot\hat{\boldsymbol{\pi}}_k\Big]\hat{v}_C(r_{jk})\Big|[R]_\iota\Big\rangle\Bigg\}. \quad (87)$$

There is no contribution for the quintet $M_S = \pm 2$ states

$$M_C^{(2,\pm 2)} = 0. \quad (88)$$

6.5. Discussion

As discussed in the introduction, we needed to evaluate the spin and isospin parts of the matrix element; since we are doing the associated calculations by brute force, we needed a complete specification of the initial and final state wavefunctions which was done in the earlier sections. We end up with a very large number of terms here resulting from the reduction of the spin and isospin factors. It would be possible to evaluate all of these terms individually to develop an estimate for the matrix element. However, since there is a great deal of redundancy at this stage, we are motivated to continue further analytic work prior to the computations in order to simplify the calculation.

7. Reduction of Spin and Isospin for the Tensor Interaction

The biggest contribution to the strong force in the Hamada–Johnston potential is from the tensor interaction. We can use Mathematica to systematically reduce the spin and isospin matrix elements also in this case.

7.1. Tensor matrix element for the singlet state

The evaluation of the tensor contribution to the matrix element leads to a result that can be expressed as

$$M_T^{(0,0)} = \frac{P}{2M}\frac{1}{(2m_{\rm av}c^2)}\sum_{j<k}\sum_{\kappa}\sum_{\iota}\Bigg\{ [R]_1\Big|\Big[-a_T^\kappa(jk;\iota)+\tilde{a}_T^\kappa(jk;\iota)\frac{z_{jk}^2}{r_{jk}^2}\Big]v_T^\kappa(r_{jk})(\hat{\mathbf{i}}_z\cdot\hat{\boldsymbol{\pi}}_j)\Big|[R]_\iota\Big\rangle$$

$$+\Big\langle [R]_1\Big|\Big[-b_T^\kappa(jk;\iota)+\tilde{b}_T^\kappa(jk;\iota)\frac{z_{jk}^2}{r_{jk}^2}\Big]\hat{v}_C(r_{jk})(\hat{\mathbf{i}}_z\cdot\hat{\boldsymbol{\pi}}_k)\Big|[R]_\iota\Big\rangle$$

$$+\Big\langle [R]_1\Big|(\hat{\mathbf{i}}_z\cdot\hat{\boldsymbol{\pi}}_j)\Big[-c_T^\kappa(jk;\iota)+\tilde{c}_T^\kappa(jk;\iota)\frac{z_{jk}^2}{r_{jk}^2}\Big]v_C^\kappa(r_{jk})\Big|[R]_\iota\Big\rangle$$

$$+\Big\langle [R]_1\Big|(\hat{\mathbf{i}}_z\cdot\hat{\boldsymbol{\pi}}_k)\Big[-d_T^\kappa(jk;\iota)+\tilde{d}_T^\kappa(jk;\iota)\frac{z_{jk}^2}{r_{jk}^2}\Big]\hat{v}_C(r_{jk})\Big|[R]_\iota\Big\rangle\Bigg\}. \quad (89)$$

Some of the expansion coefficients are identical to their central potential equivalents (for this case and also for all of the others).

$$a_T^\kappa \;=\; a_C^\kappa, \qquad b_T^\kappa \;=\; b_C^\kappa, \qquad c_T^\kappa \;=\; c_C^\kappa, \qquad d_T^\kappa \;=\; d_C^\kappa. \tag{90}$$

As mentioned above, we defer a presentation of explicit value for the expansion coefficients; later on results will be presented for the cases that are not forbidden in a different form.

7.2. Tensor matrix element for the triplet states

In the case of the triplet states, we find for $M_S = \pm 1$ that

$$\begin{aligned} M_T^{(1,\pm 1)} \;=\; \frac{P}{2M}\frac{1}{(2m_{\rm av}c^2)}\sum_{j<k}\sum_{\kappa}\sum_{\iota}\Bigg\{ & [R]_1\left|\left[-a_T^\kappa(jk;\iota)+\tilde{a}_T^\kappa(jk;\iota)\frac{z_{jk}^2}{r_{jk}^2}\right]v_T^\kappa(r_{jk})\left[(\hat{\mathbf{i}}_x \pm i\hat{\mathbf{i}}_y)\cdot\hat{\boldsymbol{\pi}}_j\right]\right|[R]_\iota\Big\rangle \\ & +\Big\langle[R]_1\left|\left[-b_T^\kappa(jk;\iota)+\tilde{b}_T^\kappa(jk;\iota)\frac{z_{jk}^2}{r_{jk}^2}\right]\hat{v}_C(r_{jk})\left[(\hat{\mathbf{i}}_x \pm i\hat{\mathbf{i}}_y)\cdot\hat{\boldsymbol{\pi}}_k\right]\right|[R]_\iota\Big\rangle \\ & +\Big\langle[R]_1\left|\left[(\hat{\mathbf{i}}_x \pm i\hat{\mathbf{i}}_y)\cdot\hat{\boldsymbol{\pi}}_j\right]\left[-c_T^\kappa(jk;\iota)+\tilde{c}_T^\kappa(jk;\iota)\frac{z_{jk}^2}{r_{jk}^2}\right]v_C^\kappa(r_{jk})\right|[R]_\iota\Big\rangle \\ & +\Big\langle[R]_1\left|\left[(\hat{\mathbf{i}}_x \pm i\hat{\mathbf{i}}_y)\cdot\hat{\boldsymbol{\pi}}_k\right]\left[-d_T^\kappa(jk;\iota)+\tilde{d}_T^\kappa(jk;\iota)\frac{z_{jk}^2}{r_{jk}^2}\right]\hat{v}_C(r_{jk})\right|[R]_\iota\Big\rangle\Bigg\}. \end{aligned} \tag{91}$$

For $M_S = 0$ the contribution vanishes

$$M_T^{(1,0)} \;=\; 0. \tag{92}$$

7.3. Tensor matrix element for the quintet states

In the case of the $M_S = 0$ quintet state we can write for the tensor contribution to the interaction matrix element

$$\begin{aligned} M_T^{(2,0)} \;=\; \frac{P}{2M}\frac{1}{(2m_{\rm av}c^2)}\sum_{j<k}\sum_{\kappa}\sum_{\iota}\Bigg\{ & [R]_1\left|\left[-a_T^\kappa(jk;\iota)+\tilde{a}_T^\kappa(jk;\iota)\frac{z_{jk}^2}{r_{jk}^2}\right]v_T^\kappa(r_{jk})(\hat{\mathbf{i}}_z\cdot\hat{\boldsymbol{\pi}}_j)\right|[R]_\iota\Big\rangle \\ & +\Big\langle[R]_1\left|\left[-b_T^\kappa(jk;\iota)+\tilde{b}_T^\kappa(jk;\iota)\frac{z_{jk}^2}{r_{jk}^2}\right]\hat{v}_C(r_{jk})(\hat{\mathbf{i}}_z\cdot\hat{\boldsymbol{\pi}}_k)\right|[R]_\iota\Big\rangle \\ & +\Big\langle[R]_1\left|(\hat{\mathbf{i}}_z\cdot\hat{\boldsymbol{\pi}}_j)\left[-c_T^\kappa(jk;\iota)+\tilde{c}_T^\kappa(jk;\iota)\frac{z_{jk}^2}{r_{jk}^2}\right]v_C^\kappa(r_{jk})\right|[R]_\iota\Big\rangle \\ & +\Big\langle[R]_1\left|(\hat{\mathbf{i}}_z\cdot\hat{\boldsymbol{\pi}}_k)\left[-d_T^\kappa(jk;\iota)+\tilde{d}_T^\kappa(jk;\iota)\frac{z_{jk}^2}{r_{jk}^2}\right]\hat{v}_C(r_{jk})\right|[R]_\iota\Big\rangle\Bigg\}. \end{aligned} \tag{93}$$

In the case of the $M_S = \pm 1$ states, we may write

$$M_T^{(2,\pm 1)} = \frac{P}{2M}\frac{1}{(2m_{\rm av}c^2)}\sum_{j<k}\sum_{\kappa}\sum_{\iota}\Bigg\{ [R]_1\Bigg|\Bigg[-a_T^\kappa(jk;\iota)+\tilde{a}_T^\kappa(jk;\iota)\frac{z_{jk}^2}{r_{jk}^2}\Bigg]v_T^\kappa(r_{jk})\Bigg[(\hat{\mathbf{i}}_x \pm i\hat{\mathbf{i}}_y)\cdot\hat{\boldsymbol{\pi}}_j\Bigg]\Bigg|[R]_\iota\Bigg\rangle$$

$$+\Bigg\langle [R]_1\Bigg|\Bigg[-b_T^\kappa(jk;\iota)+\tilde{b}_T^\kappa(jk;\iota)\frac{z_{jk}^2}{r_{jk}^2}\Bigg]\hat{v}_C(r_{jk})\Bigg[(\hat{\mathbf{i}}_x \pm i\hat{\mathbf{i}}_y)\cdot\hat{\boldsymbol{\pi}}_k\Bigg]\Bigg|[R]_\iota\Bigg\rangle$$

$$+\Bigg\langle [R]_1\Bigg|\Bigg[(\hat{\mathbf{i}}_x \pm i\hat{\mathbf{i}}_y)\cdot\hat{\boldsymbol{\pi}}_j\Bigg]\Bigg[-c_T^\kappa(jk;\iota)+\tilde{c}_T^\kappa(jk;\iota)\frac{z_{jk}^2}{r_{jk}^2}\Bigg]v_C^\kappa(r_{jk})\Bigg|[R]_\iota\Bigg\rangle$$

$$+\Bigg\langle [R]_1\Bigg|\Bigg[(\hat{\mathbf{i}}_x \pm i\hat{\mathbf{i}}_y)\cdot\hat{\boldsymbol{\pi}}_k\Bigg]\Bigg[-d_T^\kappa(jk;\iota)+\tilde{d}_T^\kappa(jk;\iota)\frac{z_{jk}^2}{r_{jk}^2}\Bigg]\hat{v}_C(r_{jk})\Bigg|[R]_\iota\Bigg\rangle\Bigg\}. \quad (94)$$

There is no contribution for $M_S = \pm 2$

$$M_T^{(2,\pm 2)} = 0. \quad (95)$$

7.4. Discussion

Similar comments can be made here as was done at the end of the previous section. The big issue here is that the tensor contribution is more complicated than the central contribution, so we end up with twice as many integrals, and these spatial integrals are going to take more effort to compute.

8. Molecular Coordinates

The evaluation of the interaction matrix element involves spin, isospin, angular momentum and multi-dimensional spatial terms. In previous sections we have dealt with the spin and isospin terms, and next we are interested in the reduction of the radial and angular part of the problem. Since there are four nucleons, each with three spatial degrees of freedom, there are in principle twelve degrees of freedom possible. The elimination of the center of mass dependence reduces this to nine degrees of freedom.

It will be convenient to implement the integrations using molecular coordinates. Two of these coordinates $\mathbf{r}_a$ and $\mathbf{r}_b$ are associated with the relative separation of the nucleons in deuterons that make up the D_2 molecule, and one $\mathbf{r}$ is the relative coordinate between the two deuterons. The nine degrees of freedom can be reduced into three radial and six angular degrees of freedom. We will have to integrate the three radial degrees of freedom numerically, and also at least one of the angular degrees of freedom. Some of the integrals will evaluate to zero due to the angular part of the integration, or due to the spatial part of the integration.

In this section we are concerned with coordinates and momentum operators, which we will use in the following sections to evaluate the spatial operators and integrals.

8.1. Molecular coordinates

To isolate the angular integration, we need to work in terms of coordinates relevant to the molecular part of the problem. We begin by defining them systematically in terms of the individual nucleon coordinates:

$$\mathbf{R} = \frac{\mathbf{r}_1 + \mathbf{r}_2 + \mathbf{r}_3 + \mathbf{r}_4}{4}, \tag{96}$$

$$\mathbf{r}_a = \mathbf{r}_2 - \mathbf{r}_1, \tag{97}$$

$$\mathbf{r}_b = \mathbf{r}_4 - \mathbf{r}_3, \tag{98}$$

$$\mathbf{r} = \frac{\mathbf{r}_3 + \mathbf{r}_4}{2} - \frac{\mathbf{r}_1 + \mathbf{r}_2}{2}. \tag{99}$$

Using these coordinates we may write for the spatial part of the D_2 wavefunction

$$R(12;34) = N_P \phi_d(r_a)\phi_d(r_b)R(r)Y_{lm}(\theta,\phi). \tag{100}$$

We see that this wavefunction does not depend on the center of mass coordinate $\mathbf{R}$, as is also the case for the ^{4}He wavefunction.

8.2. Coordinate transformations

We can specify the molecular coordinates in terms of nucleon coordinates using a matrix notation to write

$$\begin{pmatrix} \mathbf{R} \\ \mathbf{r}_a \\ \mathbf{r}_b \\ \mathbf{r} \end{pmatrix} = \begin{pmatrix} \frac{1}{4} & \frac{1}{4} & \frac{1}{4} & \frac{1}{4} \\ -1 & 1 & 0 & 0 \\ 0 & 0 & -1 & 1 \\ -\frac{1}{2} & -\frac{1}{2} & \frac{1}{2} & \frac{1}{2} \end{pmatrix} \begin{pmatrix} \mathbf{r}_1 \\ \mathbf{r}_2 \\ \mathbf{r}_3 \\ \mathbf{r}_4 \end{pmatrix}. \tag{101}$$

This can be inverted to produce

$$\begin{pmatrix} \mathbf{r}_1 \\ \mathbf{r}_2 \\ \mathbf{r}_3 \\ \mathbf{r}_4 \end{pmatrix} = \begin{pmatrix} 1 & -\frac{1}{2} & 0 & -\frac{1}{2} \\ 1 & \frac{1}{2} & 0 & -\frac{1}{2} \\ 1 & 0 & -\frac{1}{2} & \frac{1}{2} \\ 1 & 0 & \frac{1}{2} & \frac{1}{2} \end{pmatrix} \begin{pmatrix} \mathbf{R} \\ \mathbf{r}_a \\ \mathbf{r}_b \\ \mathbf{r} \end{pmatrix}. \tag{102}$$

8.3. Absence of angular momentum in the ^{4}He wavefunction

We know that the ^{4}He wavefunction has zero angular momentum associated with $\mathbf{r}$. It is helpful to seen how this happens with the ^{4}He wavefunction is written in terms of molecular coordinates. To this end, we write

$$\begin{aligned}\Phi_S(\mathbf{r}_1,\mathbf{r}_2,\mathbf{r}_3,\mathbf{r}_4) &= N_S\, u(r_{21})u(r_{31})u(r_{41})u(r_{32})u(r_{42})u(r_{43}) \\ &= N_S\, u(r_a)u\left(\left|\mathbf{r}+\frac{\mathbf{r}_a-\mathbf{r}_b}{2}\right|\right)u\left(\left|\mathbf{r}+\frac{\mathbf{r}_a+\mathbf{r}_b}{2}\right|\right)u\left(\left|\mathbf{r}-\frac{\mathbf{r}_a+\mathbf{r}_b}{2}\right|\right)u\left(\left|\mathbf{r}+\frac{\mathbf{r}_b-\mathbf{r}_a}{2}\right|\right)u(r_b). \quad (103)\end{aligned}$$

We can verify that this has no net angular momentum by considering as an example

$$\left|\mathbf{r}+\frac{\mathbf{r}_a-\mathbf{r}_b}{2}\right|^2 = |\mathbf{r}|^2+\mathbf{r}\cdot(\mathbf{r}_a-\mathbf{r}_b)+\frac{|\mathbf{r}_a-\mathbf{r}_b|^2}{4}. \quad (104)$$

Since

$$\mathbf{r}\cdot\mathbf{r}_a = \mathbf{r}\cdot\mathbf{r}_b = 0, \quad (105)$$

we may write

$$\left|\mathbf{r}+\frac{\mathbf{r}_a-\mathbf{r}_b}{2}\right|^2 = |\mathbf{r}|^2+\frac{|\mathbf{r}_a-\mathbf{r}_b|^2}{4}. \quad (106)$$

The relative distances in this case depends only on the magnitude $|\mathbf{r}|$, which means that the ^{4}He spatial wavefunction explicitly has no angular momentum associated with $\mathbf{r}$ as expected.

8.4. Relative coordinates

It is convenient to introduce nucleon coordinates with the center of mass removed

$$\boldsymbol{\xi}_j = \mathbf{r}_j-\mathbf{R}. \quad (107)$$

Note that there are only three independent coordinates since

$$\boldsymbol{\xi}_1+\boldsymbol{\xi}_2+\boldsymbol{\xi}_3+\boldsymbol{\xi}_4 = 0. \quad (108)$$

8.5. Momentum operators in terms of molecular coordinates

To isolate the angular momentum associated with the molecular coordinates, we will need to work with momentum operators written for the molecular coordinates. As an example consider $\hat{\mathbf{p}}_1$ which can be written as

$$\hat{\mathbf{p}}_1 = -i\hbar\left(\hat{\mathbf{i}}_x\frac{\partial}{\partial x_1}+\hat{\mathbf{i}}_y\frac{\partial}{\partial y_1}+\hat{\mathbf{i}}_z\frac{\partial}{\partial z_1}\right). \quad (109)$$

The derivative in x_1 can be written in terms of molecular coordinates as

$$\begin{aligned}\frac{\partial}{\partial x_1} &= \left(\frac{\partial x_a}{\partial x_1}\right)\frac{\partial}{\partial x_a} + \left(\frac{\partial x_b}{\partial x_1}\right)\frac{\partial}{\partial x_b} + \left(\frac{\partial x}{\partial x_1}\right)\frac{\partial}{\partial x} + \left(\frac{\partial X}{\partial x_1}\right)\frac{\partial}{\partial X} \\ &= (-1)\,\frac{\partial}{\partial x_a} + (0)\,\frac{\partial}{\partial x_b} + \left(-\frac{1}{2}\right)\frac{\partial}{\partial x} + \left(\frac{1}{4}\right)\frac{\partial}{\partial X}. \end{aligned} \tag{110}$$

This can be generalized to

$$\nabla_1 = (-1)\,\nabla_a + (0)\,\nabla_b + \left(-\frac{1}{2}\right)\nabla + \left(\frac{1}{4}\right)\nabla_{\mathbf{R}}, \tag{111}$$

$$\nabla_2 = (1)\,\nabla_a + (0)\,\nabla_b + \left(-\frac{1}{2}\right)\nabla + \left(\frac{1}{4}\right)\nabla_{\mathbf{R}}, \tag{112}$$

$$\nabla_3 = (0)\,\nabla_a + (-1)\,\nabla_b + \left(\frac{1}{2}\right)\nabla + \left(\frac{1}{4}\right)\nabla_{\mathbf{R}}, \tag{113}$$

$$\nabla_4 = (0)\,\nabla_a + (1)\,\nabla_b + \left(\frac{1}{2}\right)\nabla + \left(\frac{1}{4}\right)\nabla_{\mathbf{R}} \tag{114}$$

or in matrix form as

$$\begin{pmatrix}\nabla_1\\ \nabla_2\\ \nabla_3\\ \nabla_4\end{pmatrix} = \begin{pmatrix}-1 & 0 & -\frac{1}{2} & \frac{1}{4}\\ 1 & 0 & -\frac{1}{2} & \frac{1}{4}\\ 0 & -1 & \frac{1}{2} & \frac{1}{4}\\ 0 & 1 & \frac{1}{2} & \frac{1}{4}\end{pmatrix}\begin{pmatrix}\nabla_a\\ \nabla_b\\ \nabla\\ \nabla_{\mathbf{R}}\end{pmatrix}. \tag{115}$$

We can relate the momentum operators in the same way

$$\begin{pmatrix}\hat{\mathbf{p}}_1\\ \hat{\mathbf{p}}_2\\ \hat{\mathbf{p}}_3\\ \hat{\mathbf{p}}_4\end{pmatrix} = \begin{pmatrix}-1 & 0 & -\frac{1}{2} & \frac{1}{4}\\ 1 & 0 & -\frac{1}{2} & \frac{1}{4}\\ 0 & -1 & \frac{1}{2} & \frac{1}{4}\\ 0 & 1 & \frac{1}{2} & \frac{1}{4}\end{pmatrix}\begin{pmatrix}\hat{\mathbf{p}}_a\\ \hat{\mathbf{p}}_b\\ \hat{\mathbf{p}}\\ \hat{\mathbf{P}}\end{pmatrix}. \tag{116}$$

Finally, we arrive at the relations

$$\begin{aligned}\hat{\boldsymbol{\pi}}_1 &= -\hat{\mathbf{p}}_a - \frac{1}{2}\hat{\mathbf{p}}, \qquad \hat{\boldsymbol{\pi}}_2 = \hat{\mathbf{p}}_a - \frac{1}{2}\hat{\mathbf{p}},\\ \hat{\boldsymbol{\pi}}_3 &= -\hat{\mathbf{p}}_b + \frac{1}{2}\hat{\mathbf{p}}, \qquad \hat{\boldsymbol{\pi}}_4 = \hat{\mathbf{p}}_b + \frac{1}{2}\hat{\mathbf{p}}. \end{aligned} \tag{117}$$

8.6. Discussion

The $\mathbf{a} \cdot c\mathbf{P}$ interaction is expressed in terms of individual nucleon momentum operators, but we would like to do the spatial integrals in molecular coordinates. As a result, we needed the individual momentum operators expressed in terms of molecular coordinates. Now that we have the associated definitions and relations, we can work on the spatial integrals.

9. Reduction of the Spatial Integrals

We expect that some of the matrix elements will vanish because of angular momentum selection rules or because of the symmetry of the spatial wavefunctions and operators. We also expect that many of the integrals with different numbering will end up being identical, which will allow us to obtain reduced expressions to evaluate. In this section we will focus on these issues.

9.1. Reduction of one of the central potential integrals

We begin by considering the reduction of a specific integral from the singlet case of the central potential interaction

$$\left\langle [R]_1 \left| v_C^\kappa(r_{21})(\hat{\mathbf{i}}_z \cdot \hat{\boldsymbol{\pi}}_1) \right| [R]_3 \right\rangle = \int \mathrm{d}^3\mathbf{r} \int \mathrm{d}^3\mathbf{r}_a \int \mathrm{d}^3\mathbf{r}_b \, [R]_1 v_C^\kappa(r_{21})(\hat{\mathbf{i}}_z \cdot \hat{\boldsymbol{\pi}}_1)[R]_3. \tag{118}$$

To proceed we need to make clear the dependence of the different terms on the molecular coordinates. We may write

$$[R]_1 = \Phi_{4\,\mathrm{He}}(r, r_a, r_b, \theta_{ab}), \tag{119}$$

$$[R]_3 = \frac{\mathrm{e}^{-G}}{\sqrt{R_0(\Delta R)^2}} \phi_d(r_a)\phi_d(r_b)F(r)Y_{lm}(\theta, \phi), \tag{120}$$

$$r_{21} = r_a, \tag{121}$$

$$(\hat{\mathbf{i}}_z \cdot \hat{\boldsymbol{\pi}}_1) = \hat{\mathbf{i}}_z \cdot \left(-\hat{\mathbf{p}}_a - \frac{1}{2}\hat{\mathbf{p}} \right) = i\hbar \left(\frac{\mathrm{d}}{\mathrm{d}z_a} + \frac{1}{2}\frac{\mathrm{d}}{\mathrm{d}z} \right). \tag{122}$$

We see in the last of these that there will be two different two contributions to the integral, each with different selection rules. We consider first

$$-\left\langle [R]_1 \left| v_C^\kappa(r_{21})(\hat{\mathbf{i}}_z \cdot \hat{\mathbf{p}}_a) \right| [R]_3 \right\rangle = i\hbar \frac{\mathrm{e}^{-G}}{\sqrt{R_0(\Delta R)^2}} \int \mathrm{d}^3\mathbf{r} \int \mathrm{d}^3\mathbf{r}_a \int \mathrm{d}^3\mathbf{r}_b$$

$$\Phi_{4\mathrm{He}}(r, r_a, r_b, \theta_{ab}) v_C^\kappa(r_a) \left[\frac{\mathrm{d}}{\mathrm{d}z_a}\phi_d(r_a) \right] \phi_d(r_b)F(r)Y_{lm}(\theta, \phi) = 0. \tag{123}$$

Since the integrand is odd in z_a, the integral vanishes.

In the case of the other integral, we have

$$-\frac{1}{2}\left\langle [R]_1 \left| v_C^\kappa(r_{21})(\hat{\mathbf{i}}_z \cdot \hat{\mathbf{p}}) \right| [R]_3 \right\rangle = \frac{i\hbar}{2} \frac{\mathrm{e}^{-G}}{\sqrt{R_0(\Delta R)^2}} \int \mathrm{d}^3\mathbf{r} \int \mathrm{d}^3\mathbf{r}_a \int \mathrm{d}^3\mathbf{r}_b$$

$$\Phi_{4\mathrm{He}}(r, r_a, r_b, \theta_{ab}) v_C^\kappa(r_a) \phi_d(r_a) \phi_d(r_b) \left[\frac{\mathrm{d}}{\mathrm{d}z} F(r) Y_{lm}(\theta, \phi) \right]. \tag{124}$$

This integral vanishes in general for even l (in which case the integrand is odd in z), and will be nonzero only for $l = 1$ and $m = 0$. Since there are no values of S and M_S for which this integral occurs with odd l, we conclude that the integral will vanish for all cases of interest in this calculation.

$$\left\langle [R]_1 \left| v_C^\kappa(r_{21})(\hat{\mathbf{i}}_z \cdot \hat{\boldsymbol{\pi}}_1) \right| [R]_3 \right\rangle = 0 \qquad \text{for even } S. \tag{125}$$

9.2. Interpretation in terms of angular momentum

This result can be understood intuitively in terms of angular momentum. The operator in this case can be understood as having one unit of angular momentum by virtue of the appearance of $(\hat{\mathbf{i}}_z \cdot \hat{\boldsymbol{\pi}}_1)$. Since $\hat{\boldsymbol{\pi}}$ can be decomposed into $-\hat{\mathbf{p}}_a - \hat{\mathbf{p}}/2$, we can say that this unit of angular momentum can apply either to the relative degree of freedom within the first deuteron, or the relative molecule degree of freedom. We can think of

$$v_C^\kappa(r_{21})(\hat{\mathbf{i}}_z \cdot \hat{\boldsymbol{\pi}}_1)$$

in this context as a generalized dipole operator.

The internal deuteron part of the dipole gives no contribution. In the approximation under consideration we model the deuteron using only a spherically symmetric wavefunction $\phi_d(r_a)$, so it has s-symmetry. The ground state ^{4}He wavefunction in this approximation is a four-nucleon correlated ^{1}S wavefunction which has no net angular momentum. It is not the case that there is no angular momentum present associated with the relative $\mathbf{r}_a$ degree of freedom, since the four-nucleon wavefunction is correlated. Instead, the a and b channels are correlated so that when the a channel has one unit of angular momentum (which would lead to a finite integral in $\mathbf{r}_a$), so does the b channel (producing a vanishing integral).

9.3. Selection rule for central potential contributions

We can generalize this argument into a selection rule

$$\left\langle [R]_1 \left| v_C^\kappa(r_{21})(\hat{\mathbf{i}}_z \cdot \hat{\boldsymbol{\pi}}_1) \right| [R]_3 \right\rangle \neq 0 \qquad \text{for } S = 1;\ M_S = \pm 1;\ l = 1;\ m = \mp 1. \tag{126}$$

A further generalization to the other integrals appearing in the central potential contribution to the interaction would lead us to the conclusion

$$M_C = 0 \qquad \text{for all cases except } S = 1;\ M_S = \pm 1;\ l = 1;\ m = \mp 1. \tag{127}$$

9.4. Reduction in the case of an allowed transition

This motivates us to examine the evaluation of a spatial integral under conditions where a finite result is expected. In this case, we consider

$$\left\langle [R]_1 \left| v_C^\kappa(r_{jk}) \left[(\hat{\mathbf{i}}_x \pm i\hat{\mathbf{i}}_y)\cdot\hat{\boldsymbol{\pi}}_1 \right] \right| [R]_3 \right\rangle = \int \mathrm{d}^3\mathbf{r} \int \mathrm{d}^3\mathbf{r}_a \int \mathrm{d}^3\mathbf{r}_b [R]_1 v_C^\kappa(r_{12}) \left[(\hat{\mathbf{i}}_x \pm i\hat{\mathbf{i}}_y)\cdot\hat{\boldsymbol{\pi}}_1 \right] [R]_3. \tag{128}$$

Following the arguments given above, we can immediately reduce it to

$$\left\langle [R]_1 \left| v_C^\kappa(r_{jk}) \left[(\hat{\mathbf{i}}_x \pm i\hat{\mathbf{i}}_y)\cdot\hat{\boldsymbol{\pi}}_1 \right] \right| [R]_3 \right\rangle = \frac{i\hbar}{2} \frac{\mathrm{e}^{-G}}{\sqrt{R_0(\Delta R)^2}} \int \mathrm{d}^3\mathbf{r} \int \mathrm{d}^3\mathbf{r}_a \int \mathrm{d}^3\mathbf{r}_b$$

$$\Phi_{4\mathrm{He}}(r, r_a, r_b, \theta_{ab}) v_C^\kappa(r_a)\phi_d(r_a)\phi_d(r_b) \left[\left(\frac{\mathrm{d}}{\mathrm{d}x} \pm i\frac{\mathrm{d}}{\mathrm{d}y} \right) F(r) Y_{l,\mp 1}(\theta,\phi) \right]. \tag{129}$$

We can evaluate the derivatives for $l = 1$ to obtain

$$\left(\frac{\mathrm{d}}{\mathrm{d}x} \pm i\frac{\mathrm{d}}{\mathrm{d}y} \right) F(r) Y_{1,\mp 1}(\theta,\phi) = \pm\sqrt{\frac{3}{8\pi}} \left[\frac{r^2+z^2}{r^3} + \frac{r^2-z^2}{r^2}\frac{\mathrm{d}}{\mathrm{d}r} \right] F(r). \tag{130}$$

We can use this to write the integral in terms of radial and angular integrals to give

$$\begin{aligned} \left\langle [R]_1 \left| v_C^\kappa(r_{jk}) \left[(\hat{\mathbf{i}}_x \pm i\hat{\mathbf{i}}_y)\cdot\hat{\boldsymbol{\pi}}_1 \right] \right| [R]_3 \right\rangle = {} & \frac{i\hbar}{2} \frac{\mathrm{e}^{-G}}{\sqrt{R_0(\Delta R)^2}} 16\pi^3 \int_0^\infty r^2\mathrm{d}r \int_0^\infty r_a^2\mathrm{d}r_a \int_0^\infty r_b^2\mathrm{d}r_b \\ & \int_0^\pi \sin\theta_{ab}\,\mathrm{d}\theta_{ab}\ \Phi_{4\mathrm{He}}(r, r_a, r_b, \theta_{ab}) v_C^\kappa(r_a)\phi_d(r_a)\phi_d(r_b) \\ & \int_0^\pi \sin\theta\,\mathrm{d}\theta \left[\pm\sqrt{\frac{3}{8\pi}} \left[\frac{1+\cos^2\theta}{r} + \sin^2\theta\frac{\mathrm{d}}{\mathrm{d}r} \right] F(r) \right]. \end{aligned} \tag{131}$$

We integrate over θ to obtain

$$\left\langle [R]_1 \left| v_C^\kappa(r_{jk}) \left[(\hat{\mathbf{i}}_x \pm i\hat{\mathbf{i}}_y)\cdot\hat{\boldsymbol{\pi}}_1 \right] \right| [R]_3 \right\rangle = \pm\frac{i\hbar}{2} \frac{\mathrm{e}^{-G}}{\sqrt{R_0(\Delta R)^2}} 16\pi^3 \sqrt{\frac{8}{3\pi}} \int_0^\infty r^2\mathrm{d}r \int_0^\infty r_a^2\mathrm{d}r_a \int_0^\infty r_b^2\mathrm{d}r_b$$

$$\int_0^\pi \sin\theta_{ab}\,\mathrm{d}\theta_{ab}\ \Phi_{4\mathrm{He}}(r, r_a, r_b, \theta_{ab}) v_C^\kappa(r_a)\phi_d(r_a)\phi_d(r_b) \left(\frac{1}{r} + \frac{1}{2}\frac{\mathrm{d}}{\mathrm{d}r} \right) F(r). \tag{132}$$

The four-dimensional integral that results can be done numerically easily; selected numerical results are listed in Table 4.

Table 4. Numerical values for four dimensional central potential integrals; units are MeV/fm.

Integral	Prefactor	eS	eT	oS	oT
$\left\langle [R]_1 \left\| v_C^\kappa(r_{21})(\hat{\mathbf{i}}_x \pm i\hat{\mathbf{i}}_y)\cdot\hat{\boldsymbol{\pi}}_1 \right\| [R]_3 \right\rangle$	$i\hbar e^{-G}$	1.24×10^{-3}	5.45×10^{-4}	1.36×10^{-4}	-3.12×10^{-4}
$\left\langle [R]_1 \left\| v_C^\kappa(r_{31})(\hat{\mathbf{i}}_x \pm i\hat{\mathbf{i}}_y)\cdot\hat{\boldsymbol{\pi}}_1 \right\| [R]_3 \right\rangle$	$i\hbar e^{-G}$	4.00×10^{-4}	2.43×10^{-4}	1.50×10^{-5}	-7.85×10^{-5}
$\left\langle [R]_1 \left\| v_C^\kappa(r_{41})(\hat{\mathbf{i}}_x \pm i\hat{\mathbf{i}}_y)\cdot\hat{\boldsymbol{\pi}}_1 \right\| [R]_3 \right\rangle$	$i\hbar e^{-G}$	4.00×10^{-4}	2.43×10^{-4}	1.50×10^{-5}	-7.85×10^{-5}

9.5. Checking the $l = 3$ case

It may not be obvious that a strict dipole selection rule is obeyed for this integral, so this motivates us to examine the integral for the next odd l. For $l = 3$ we may write

$$\left(\frac{\mathrm{d}}{\mathrm{d}x} \pm i\frac{\mathrm{d}}{\mathrm{d}y}\right) F(r) Y_{3,\mp1}(\theta,\phi) \;=\; \mp\frac{1}{8}\sqrt{\frac{21}{\pi}}\left[\frac{r^4+6r^2z^2-15z^4}{r^5} + \frac{r^4-6z^2r^2+5z^4}{r^4}\frac{\mathrm{d}}{\mathrm{d}r}\right]F(r). \tag{133}$$

We can use this to write for the integral

$$\begin{aligned}
&\left\langle [R]_1 \left| v_C^\kappa(r_{jk})\left[(\hat{\mathbf{i}}_x \pm i\hat{\mathbf{i}}_y)\cdot\hat{\boldsymbol{\pi}}_j\right] \right| [R]_3 \right\rangle \\
&\qquad = \;\mp\frac{i\hbar}{2}\frac{e^{-G}}{\sqrt{R_0(\Delta R)^2}} 16\pi^3 \frac{1}{8}\sqrt{\frac{21}{\pi}} \int_0^\infty r^2\mathrm{d}r \int_0^\infty r_a^2\mathrm{d}r_a \int_0^\infty r_b^2\mathrm{d}r_b \\
&\int_0^\pi \sin\theta_{ab}\,\mathrm{d}\theta_{ab}\;\Phi_{4\mathrm{He}}(r,r_a,r_b,\theta_{ab}) v_C^\kappa(r_a)\phi_d(r_a)\phi_d(r_b) \\
&\int_0^\pi \sin\theta\,\mathrm{d}\theta\left[\frac{1+6\cos^2\theta-15\cos^4\theta}{r} + (1-6\cos^2\theta+5\cos^4\theta)\frac{\mathrm{d}}{\mathrm{d}r}\right]F(r).
\end{aligned} \tag{134}$$

We evaluate the θ integral to obtain

$$\left\langle [R]_1 \left| v_C^\kappa(r_{jk})\left[(\hat{\mathbf{i}}_x \pm i\hat{\mathbf{i}}_y)\cdot\hat{\boldsymbol{\pi}}_j\right] \right| [R]_3 \right\rangle \;=\; 0. \tag{135}$$

This supports the notion that a dipole selection rule is appropriate for the integral under discussion.

9.6. Symmetry in the spatial integrals

In the numerical results of Table 4 we see that the same numerical values show up for different cases, which motivates us to examine this issue further in the hope that we can simplify things. In general we find that for integrals involving the spatial function $[R]_3$ we get the same magnitude when the two nucleons are in different deuterons (which would occur for the r_{31}, r_{41}, r_{32} and r_{42} cases). If the two nucleons are in the same deuteron (the r_{21} and r_{43} cases) the magnitude is again the same.

We expect a sign difference when $\hat{\boldsymbol{\pi}}_1$ and $\hat{\boldsymbol{\pi}}_2$ appear in the integrand for an $[R]_3$ integral as compared with when $\hat{\boldsymbol{\pi}}_3$ and $\hat{\boldsymbol{\pi}}_4$ show up. This is because of the different dependence on $\hat{\mathbf{p}}$ that appears in Eq. (117). In the case of integrals with $[R]_4$ and $[R]_5$, the nucleons which are in the same deuteron change. We again would expect the the integral to have the same magnitude for the two cases (nucleons in the same deuteron, or in different deuterons).

9.7. Separation of spatial integrals

It will be convenient to take advantage of the separation

$$\left\langle [R]_1 \left| \left[(\hat{\mathbf{i}}_x \pm i\hat{\mathbf{i}}_y)\cdot\hat{\boldsymbol{\pi}}_j \right] v_C^\kappa(r_{jk}) \right| [R]_\iota \right\rangle = \left\langle [R]_1 \left| \left\{ \left[(\hat{\mathbf{i}}_x \pm i\hat{\mathbf{i}}_y)\cdot\hat{\boldsymbol{\pi}}_j \right] v_C^\kappa(r_{jk}) \right\} \right| [R]_\iota \right\rangle + \left\langle [R]_1 \left| v_C^\kappa(r_{jk}) \left[(\hat{\mathbf{i}}_x \pm i\hat{\mathbf{i}}_y)\cdot\hat{\boldsymbol{\pi}}_j \right] \right| [R]_\iota \right\rangle. \tag{136}$$

We see that the second integral that appears on the RHS is of the same form as we have been considering above. This suggests that it should be possible to write for the overall expression

$$\begin{aligned} M_C^{(1,\pm1)} = \frac{P}{2M}\frac{1}{(2m_{\rm av}c^2)}\sum_{j<k}\sum_\kappa\sum_\iota \Bigg\{ & [a_C^\kappa(jk;\iota)+c_C^\kappa(jk;\iota)]\left\langle [R]_1 \left| v_C^\kappa(r_{jk})\left[(\hat{\mathbf{i}}_x \pm i\hat{\mathbf{i}}_y)\cdot\hat{\boldsymbol{\pi}}_j \right] \right| [R]_\iota \right\rangle \\ & + [b_C^\kappa(jk;\iota)+d_C^\kappa(jk;\iota)]\left\langle [R]_1 \left| \hat{v}_C(r_{jk})\left[(\hat{\mathbf{i}}_x \pm i\hat{\mathbf{i}}_y)\cdot\hat{\boldsymbol{\pi}}_k \right] \right| [R]_\iota \right\rangle \\ & + c_C^\kappa(jk;\iota)\left\langle [R]_1 \left| \left[\left((\hat{\mathbf{i}}_x \pm i\hat{\mathbf{i}}_y)\cdot\hat{\boldsymbol{\pi}}_j \right) v_C^\kappa(r_{jk}) \right] \right| [R]_\iota \right\rangle \\ & + d_C^\kappa(jk;\iota)\left\langle [R]_1 \left| \left[\left((\hat{\mathbf{i}}_x \pm i\hat{\mathbf{i}}_y)\cdot\hat{\boldsymbol{\pi}}_k \right) \hat{v}_C(r_{jk}) \right] \right| [R]_\iota \right\rangle \Bigg\} \end{aligned} \tag{137}$$

and then simplify it to

$$\begin{aligned} M_C^{(1,\pm1)} = \frac{P}{2M}\frac{1}{(2m_{\rm av}c^2)}\sum_\kappa \Bigg\{ & A_C^\kappa\left\langle [R]_1 \left| v_C^\kappa(r_{21})\left[(\hat{\mathbf{i}}_x \pm i\hat{\mathbf{i}}_y)\cdot\hat{\boldsymbol{\pi}}_1 \right] \right| [R]_3 \right\rangle \\ & + B_C^\kappa\left\langle [R]_1 \left| \hat{v}_C(r_{31})\left[(\hat{\mathbf{i}}_x \pm i\hat{\mathbf{i}}_y)\cdot\hat{\boldsymbol{\pi}}_1 \right] \right| [R]_3 \right\rangle \\ & C_C^\kappa\left\langle [R]_1 \left| \left[\left((\hat{\mathbf{i}}_x \pm i\hat{\mathbf{i}}_y)\cdot\hat{\boldsymbol{\pi}}_1 \right) v_C^\kappa(r_{21}) \right] \right| [R]_3 \right\rangle \\ & + D_C^\kappa\left\langle [R]_1 \left| \left[\left((\hat{\mathbf{i}}_x \pm i\hat{\mathbf{i}}_y)\cdot\hat{\boldsymbol{\pi}}_1 \right) \hat{v}_C(r_{31}) \right] \right| [R]_3 \right\rangle \Bigg\}. \end{aligned} \tag{138}$$

Written in this form, we see that the matrix element is made up of 16 individual terms.

9.8. Expressions for the expansion coefficients

To proceed, we require expressions for the expansion coefficients. It seems reasonably clear how to identify the same deuteron and different deuteron cases when dealing with integrals involving $[R]_4$ and $[R]_5$; for example we may write

$$\left\langle [R]_1 \left| v_C^\kappa(r_{21}) \left[(\hat{\mathbf{i}}_x \pm i\hat{\mathbf{i}}_y) \cdot \hat{\boldsymbol{\pi}}_1 \right] \right| [R]_4 \right\rangle = \left\langle [R]_1 \left| v_C^\kappa(r_{31}) \left[(\hat{\mathbf{i}}_x \pm i\hat{\mathbf{i}}_y) \cdot \hat{\boldsymbol{\pi}}_1 \right] \right| [R]_3 \right\rangle, \tag{139}$$

since r_{21} involves nucleons in different deuterons for the spatial wavefunction $[R]_4 = R(13;24)$. A more subtle case is

$$\begin{aligned} \left\langle [R]_1 \left| v_C^\kappa(r_{21}) \left[(\hat{\mathbf{i}}_x \pm i\hat{\mathbf{i}}_y) \cdot \hat{\boldsymbol{\pi}}_2 \right] \right| [R]_4 \right\rangle &= \left\langle [R]_1 \left| v_C^\kappa(r_{31}) \left[(\hat{\mathbf{i}}_x \pm i\hat{\mathbf{i}}_y) \cdot \hat{\boldsymbol{\pi}}_3 \right] \right| [R]_3 \right\rangle \\ &= -\left\langle [R]_1 \left| v_C^\kappa(r_{31}) \left[(\hat{\mathbf{i}}_x \pm i\hat{\mathbf{i}}_y) \cdot \hat{\boldsymbol{\pi}}_1 \right] \right| [R]_3 \right\rangle. \end{aligned} \tag{140}$$

The idea here is that we first renumber the nucleons in order to change $[R]_4$ into $[R]_3$, and then note that a sign change occurs for the $\hat{\mathbf{p}}$ part of $\hat{\boldsymbol{\pi}}_3$ and $\hat{\boldsymbol{\pi}}_1$.

We can use the arguments given above to develop explicit expressions for the expansion coefficients. We may write

$$\begin{aligned} A_C^\kappa = {} & a_C(12;3) - a_C(34;3) - b_C(12;3) + b_C(34;3) \\ & + a_C(13;4) - a_C(24;4) - b_C(13;4) + b_C(24;4) \\ & + a_C(14;5) - a_C(23;5) - b_C(14;5) + b_C(23;5) \\ & + c_C(12;3) - c_C(34;3) - d_C(12;3) + d_C(34;3) \\ & + c_C(13;4) - c_C(24;4) - d_C(13;4) + d_C(24;4) \\ & + c_C(14;5) - c_C(23;5) - d_C(14;5) + d_C(23;5), \end{aligned} \tag{141}$$

$$\begin{aligned} B_C^\kappa = {} & a_C(13;3) + a_C(14;3) + a_C(23;3) + a_C(24;3) \\ & - b_C(13;3) - b_C(14;3) - b_C(23;3) - b_C(24;3) \\ & + a_C(12;4) + a_C(14;4) + a_C(32;4) + a_C(34;4) \\ & - b_C(12;4) - b_C(14;4) - b_C(32;4) - b_C(34;4) \\ & + a_C(12;5) + a_C(13;5) + a_C(42;5) + a_C(43;5) \\ & - b_C(12;5) - b_C(13;5) - b_C(42;5) - b_C(43;5) \\ & c_C(13;3) + c_C(14;3) + c_C(23;3) + c_C(24;3) \\ & - d_C(13;3) - d_C(14;3) - d_C(23;3) - d_C(24;3) \\ & + c_C(12;4) + c_C(14;4) + c_C(32;4) + c_C(34;4) \\ & - d_C(12;4) - d_C(14;4) - d_C(32;4) - d_C(34;4) \\ & + c_C(12;5) + c_C(13;5) + c_C(42;5) + c_C(43;5) \\ & - d_C(12;5) - d_C(13;5) - d_C(42;5) - d_C(43;5), \end{aligned} \tag{142}$$

$$C_C^\kappa = c_C(12;3) - c_C(34;3) + c_C(13;4) - c_C(24;4) + c_C(14;5) - c_C(23;5), \tag{143}$$

$$\begin{aligned} D_C^\kappa &= d_C(13;3) + d_C(14;3) + d_C(23;3) + d_C(24;3) \\ &\quad d_C(12;4) + d_C(14;4) + d_C(32;4) + d_C(34;4) \\ &\quad d_C(12;5) + d_C(13;5) + d_C(42;5) + d_C(43;5). \end{aligned} \tag{144}$$

We draw attention to the ordering of the first two indices in these expressions, since the sign depends on the order.

9.9. Discussion

When we first carried out the reduction of the spin and isospin parts of the matrix elements, we ended up with a very large number of terms. Here we have recognized that many of the associated spatial integrals are zero (on account of angular momentum selection rules), and that the ones that are left are in many cases numerically identical. This allowed us to combine together all the terms that are the same, leading to a dramatic simplification of the overall calculation.

10. Evaluation of the Interaction Matrix Element

We can use the approach outlined above to carry out a systematic evaluation of the interaction matrix element. For each of the interactions, we need to first determine which terms are non-zero, evaluate the associated expansion coefficients, evaluate the associated spatial integrals, and then sum the results.

10.1. Central potential contribution for $l = 1$

In the case of the central potential we may write

$$M_C^{(1,\pm 1)} = (cP)\left[\mathrm{e}^{-G}\sqrt{\frac{R_0}{\langle R\rangle}\frac{(\Delta R)^2}{\langle(\Delta R)^2\rangle}}\right]_{l=1}\sum_\kappa A_C^\kappa I_C^\kappa + B_C^\kappa J_C^\kappa + C_C^\kappa K_C^\kappa + D_C^\kappa L_C^\kappa. \tag{145}$$

Results for the expansion coefficients from Mathematica are presented in Table 5. For the spatial integrals $I_C^\kappa(l,m), \cdots$ we may write

$$\begin{aligned} I_C^\kappa(1,\mp 1) &= \frac{1}{2Mc}\frac{1}{(2m_{\mathrm{av}}c^2)}\left\langle [R]_1 \left| v_C^\kappa(r_{21})\left[(\hat{\mathbf{i}}_x \pm \hat{\mathbf{i}}_y)\cdot\hat{\boldsymbol{\pi}}_1\right]\right| \phi_d(r_{21})\phi_d(r_{43})\frac{F(r)}{\sqrt{R_0(\Delta R)^2}}Y_{1,\mp 1}(\theta,\phi)\right\rangle \\ &= \pm\,\mathrm{Const}\int_0^\infty r^2\mathrm{d}r\int \mathrm{d}^3\mathbf{r}_a\int \mathrm{d}^3\mathbf{r}_b\ \Phi_{4\mathrm{He}}(r,r_a,r_b,\theta_{ab})\phi_d(r_a)\phi_d(r_b)v_C^\kappa(r_a)\sqrt{\frac{8\pi}{3}}\left[\frac{2}{r}+\frac{\mathrm{d}}{\mathrm{d}r}\right]F(r), \end{aligned} \tag{146}$$

$$\begin{aligned} J_C^\kappa(1,\mp 1) &= \frac{1}{2Mc}\frac{1}{(2m_{\mathrm{av}}c^2)}\left\langle [R]_1 \left| v_C^\kappa(r_{31})\left[(\hat{\mathbf{i}}_x \pm i\hat{\mathbf{i}}_y)\cdot\hat{\boldsymbol{\pi}}_1\right]\right| \phi_d(r_{21})\phi_d(r_{43})\frac{F(r)}{\sqrt{R_0(\Delta R)^2}}Y_{1,\mp 1}(\theta,\phi)\right\rangle \\ &= \pm\,\mathrm{Const}\int_0^\infty r^2\mathrm{d}r\int \mathrm{d}^3\mathbf{r}_a\int \mathrm{d}^3\mathbf{r}_b\ \Phi_{4\mathrm{He}}(r,r_a,r_b,\theta_{ab})\phi_d(r_a)\phi_d(r_b)v_C^\kappa(r_{31})\sqrt{\frac{8\pi}{3}}\left[\frac{2}{r}+\frac{\mathrm{d}}{\mathrm{d}r}\right]F(r), \end{aligned} \tag{147}$$

$$\begin{aligned} K_C^\kappa(1,\mp 1) &= \frac{1}{2Mc}\frac{1}{(2m_{\mathrm{av}}c^2)}\left\langle [R]_1 \left| \left\{(\hat{\mathbf{i}}_x \pm i\hat{\mathbf{i}}_y)\cdot\hat{\boldsymbol{\pi}}_1 v_C^\kappa(r_{21})\right\}\right| \phi_d(r_{21})\phi_d(r_{43})\frac{F(r)}{\sqrt{R_0(\Delta R)^2}}Y_{1,\mp 1}(\theta,\phi)\right\rangle \\ &= 0, \end{aligned} \tag{148}$$

Table 5. Expansion coefficients for the central potential contribution to the interaction matrix element for $S = 1$ and $M_S = \pm 1$.

Coefficient	eS	eT	oS	oT
A_C^κ	$-\frac{1}{16\sqrt{2}}$	$-\frac{23}{16\sqrt{2}}$	$\frac{69}{16\sqrt{2}}$	$\frac{1}{48\sqrt{2}}$
B_C^κ	0	$-\frac{13}{8\sqrt{2}}$	0	$\frac{35}{24\sqrt{2}}$
C_C^κ	$\frac{1}{16\sqrt{2}}$	$\frac{23}{16\sqrt{2}}$	$-\frac{69}{16\sqrt{2}}$	$-\frac{1}{48\sqrt{2}}$
D_C^κ	0	$\frac{13}{8\sqrt{2}}$	0	$-\frac{35}{24\sqrt{2}}$

$$L_C^\kappa(1,\mp 1) = \frac{1}{2Mc}\frac{1}{(2m_{\rm av}c^2)}\left\langle [R]_1 \left| \left\{ (\hat{\mathbf{i}}_x \pm i\hat{\mathbf{i}}_y)\cdot \hat{\boldsymbol{\pi}}_1 v_C^\kappa(r_{31}) \right\} \right| \phi_d(r_{21})\phi_d(r_{43}) \frac{F(r)}{\sqrt{R_0(\Delta R)^2}} Y_{1,\mp 1}(\theta,\phi) \right\rangle$$
$$= \pm \text{Const} \int_0^\infty r^2 \mathrm{d}r \int \mathrm{d}^3\mathbf{r}_a \int \mathrm{d}^3\mathbf{r}_b \; \Phi_{4\text{He}}(r, r_a, r_b, \theta_{ab})\phi_d(r_a)\phi_d(r_b)F(r)\sqrt{\frac{8\pi}{3}}\frac{r}{r_{31}}\frac{\mathrm{d}}{\mathrm{d}r_{31}}v_C^\kappa(r_{31}), \quad (149)$$

where

$$\text{Const} = \frac{i\hbar}{2}\frac{1}{2Mc}\frac{1}{(2m_{\rm av}c^2)}\frac{1}{\sqrt{R_0(\Delta R)^2}}. \quad (150)$$

We can use the results for the expansion coefficients along with the numerical results for the spatial integrals in Table 6 to obtain

Table 6. Dimensionless spatial integrals for the central potential contribution to the interaction matrix element for the case $S = 1$, $M_S = 1$, $l = 1$, $m = -1$; the integrals for the other case with $M_S = -1$ and $m = 1$ differ only in sign.

Integral	eS	eT	oS	oT
I_C^κ	$i\ 3.48 \times 10^{-8}$	$i\ 1.53 \times 10^{-8}$	$i\ 3.81 \times 10^{-9}$	$-i\ 8.75 \times 10^{-9}$
J_C^κ	$i\ 1.12 \times 10^{-8}$	$i\ 6.80 \times 10^{-9}$	$i\ 4.20 \times 10^{-10}$	$-i\ 2.20 \times 10^{-9}$
K_C^κ	0	0	0	0
L_C^κ	$-i\ 8.81 \times 10^{-9}$	$-i\ 4.53 \times 10^{-9}$	$-i\ 1.34 \times 10^{-11}$	$i\ 2.63 \times 10^{-9}$

$$M_C^{(S,M_S)} = \left[e^{-G\sqrt{\frac{R_0}{\langle R\rangle}\frac{(\Delta R)^2}{\langle(\Delta R)^2\rangle}}} \right]_{l=1} \times \begin{cases} i(cP)\,2.35\times10^{-8} & S=1,\ M_S=-1,\ l=1,\ m=\ 1 \\ 0 & S=1,\ M_S=\ 0,\ l=1,\ m=\ 0 \\ -i(cP)\,2.35\times10^{-8} & S=1,\ M_S=\ 1,\ l=1,\ m=-1 \end{cases} \quad (151)$$

10.2. Tensor potential contribution for $l = 1$

In the case of the tensor potential we may write

$$M_T^{(1,\pm1)} = (cP)\left[e^{-G\sqrt{\frac{R_0}{\langle R\rangle}\frac{(\Delta R)^2}{\langle(\Delta R)^2\rangle}}} \right]_{l=1} \sum_\kappa A_T^\kappa I_T^\kappa + B_T^\kappa J_T^\kappa + C_T^\kappa K_T^\kappa + D_T^\kappa L_T^\kappa + \tilde{A}_T^\kappa \tilde{I}_T^\kappa + \tilde{B}_T^\kappa \tilde{J}_T^\kappa + \tilde{C}_T^\kappa \tilde{K}_T^\kappa + \tilde{D}_T^\kappa \tilde{L}_T^\kappa. \quad (152)$$

The expansion coefficients A_T through D_T can be related to the expansion coefficients of the central potential case

$$A_T^\kappa = -A_C^\kappa, \qquad B_T^\kappa = -B_C^\kappa, \qquad C_T^\kappa = -C_C^\kappa, \qquad D_T^\kappa = -D_C^\kappa. \quad (153)$$

We have used Mathematica to sum contributions for the other coefficients; the results are tabulated in Table 7.

Table 7. Expansion coefficients for the tensor potential contribution to the interaction matrix element for $S = 1$ and $M_S = \pm1$.

Coefficient	eS	eT	oS	oT
$\tilde{A}_C^\kappa$	$-\frac{1}{16\sqrt{2}}$	$-\frac{69}{16\sqrt{2}}$	$\frac{69}{16\sqrt{2}}$	$\frac{1}{16\sqrt{2}}$
$\tilde{B}_C^\kappa$	0	$-\frac{45}{4\sqrt{2}}$	0	$\frac{51}{4\sqrt{2}}$
$\tilde{C}_C^\kappa$	$\frac{1}{16\sqrt{2}}$	$\frac{69}{16\sqrt{2}}$	$-\frac{69}{16\sqrt{2}}$	$-\frac{1}{16\sqrt{2}}$
$\tilde{D}_C^\kappa$	0	$-\frac{15}{4\sqrt{2}}$	0	$-\frac{17}{4\sqrt{2}}$

The spatial integrals $I_T^\kappa, \cdots L_T^\kappa$ have a form very similar to that of the central potential integrals; for example, we may write

$$I_T^\kappa(1,\mp1) = \frac{1}{2Mc}\frac{1}{(2m_{\rm av}c^2)}\left\langle [R]_1 \left| v_T^\kappa(r_{21}) \left[(\hat{\mathbf{i}}_x \pm \hat{\mathbf{i}}_y)\cdot\hat{\boldsymbol{\pi}}_1 \right] \right| \phi_d(r_{21})\phi_d(r_{43}) \frac{F(r)}{\sqrt{R_0(\Delta R)^2}} Y_{1,\mp1}(\theta,\phi) \right\rangle$$
$$= \pm\,\text{Const}\int_0^\infty r^2 dr \int d^3\mathbf{r}_a \int d^3\mathbf{r}_b\ \Phi_{4\rm He}(r, r_a, r_b, \theta_{ab})\phi_d(r_a)\phi_d(r_b) v_T^\kappa(r_a)\sqrt{\frac{8\pi}{3}}\left[\frac{2}{r} + \frac{d}{dr}\right]F(r) \quad (154)$$

with analogous modifications of the other cases. Results for the four-dimensional numerical integrations are given in Table 8.

Table 8. Dimensionless spatial integrals for the tensor potential contribution to the interaction matrix element for $S = 1$, $M_S = 1$, $l = 1$ and $m = -1$; the matrix elements for the other case with $M_S = -1$ and $m = 1$ differ only by a sign.

Integral	eS	eT	oS	oT
I_T^κ	$i\ 3.66 \times 10^{-8}$	$i\ 2.94 \times 10^{-8}$	$i\ 3.66 \times 10^{-8}$	$i\ 1.88 \times 10^{-8}$
J_T^κ	$i\ 1.57 \times 10^{-8}$	$i\ 1.39 \times 10^{-8}$	$i\ 1.57 \times 10^{-8}$	$i\ 1.10 \times 10^{-8}$
K_T^κ	0	0	0	0
L_T^κ	$-i\ 1.06 \times 10^{-8}$	$-i\ 8.84 \times 10^{-9}$	$-i\ 1.06 \times 10^{-8}$	$-i\ 6.20 \times 10^{-9}$

The other spatial integrals can be written as

$$\begin{aligned}\tilde{I}_T^\kappa(1,\mp 1) &= \frac{1}{2Mc}\frac{1}{(2m_{\rm av}c^2)}\left\langle [R]_1 \left| \frac{z_{21}^2}{r_{21}^2} v_T^\kappa(r_{21}) \left[(\hat{\mathbf{i}}_x \pm \hat{\mathbf{i}}_y)\cdot \hat{\boldsymbol{\pi}}_1 \right] \right| \phi_d(r_{21})\phi_d(r_{43}) \frac{F(r)}{\sqrt{R_0(\Delta R)^2}} Y_{1,\mp 1}(\theta,\phi) \right\rangle \\ &= \pm \text{Const} \int_0^\infty r^2 \mathrm{d}r \int \mathrm{d}^3\mathbf{r}_a \int \mathrm{d}^3\mathbf{r}_b\ \Phi_{4\rm He}(r, r_a, r_b, \theta_{ab})\phi_d(r_a)\phi_d(r_b) \frac{z_{21}^2}{r_{21}^2} v_T^\kappa(r_a) \sqrt{\frac{8\pi}{3}} \left[\frac{2}{r} + \frac{\mathrm{d}}{\mathrm{d}r} \right] F(r), \quad (155)\end{aligned}$$

$$\begin{aligned}\tilde{J}_T^\kappa(1,\mp 1) &= \frac{1}{2Mc}\frac{1}{(2m_{\rm av}c^2)}\left\langle [R]_1 \left| \frac{z_{31}^2}{r_{31}^2} v_T^\kappa(r_{31}) \left[(\hat{\mathbf{i}}_x \pm \hat{\mathbf{i}}_y)\cdot \hat{\boldsymbol{\pi}}_1 \right] \right| \phi_d(r_{21})\phi_d(r_{43}) \frac{F(r)}{\sqrt{R_0(\Delta R)^2}} Y_{1,\mp 1}(\theta,\phi) \right\rangle \\ &= \pm \text{Const} \int_0^\infty r^2 \mathrm{d}r \int \mathrm{d}^3\mathbf{r}_a \int \mathrm{d}^3\mathbf{r}_b\ \Phi_{4\rm He}(r, r_a, r_b, \theta_{ab})\phi_d(r_a)\phi_d(r_b) v_T^\kappa(r_{31}) \\ &\quad \sqrt{\frac{8\pi}{3}} \left[\left(\frac{4}{5}\frac{r}{r_{31}^2} + \frac{1}{2}\frac{z_{ab}^2}{r r_{31}^2} \right) + \left(\frac{1}{5}\frac{r^2}{r_{31}^2} + \frac{1}{4}\frac{z_{ab}^2}{r_{31}^2} \right) \frac{\mathrm{d}}{\mathrm{d}r} \right] F(r), \quad (156)\end{aligned}$$

$$\begin{aligned}\tilde{K}_T^\kappa(1,\mp 1) &= \frac{1}{2Mc}\frac{1}{(2m_{\rm av}c^2)}\left\langle [R]_1 \left| \left[(\hat{\mathbf{i}}_x \pm i\hat{\mathbf{i}}_y)\cdot \hat{\boldsymbol{\pi}}_1 v_T^\kappa(r_a) \frac{z_a^2}{r_a^2} \right] \right| \phi_d(r_a)\phi_d(r_b) \frac{F(r)}{\sqrt{R_0(\Delta R)^2}} Y_{1,\mp 1}(\theta,\phi) \right\rangle \\ &= 0, \quad (157)\end{aligned}$$

$$\begin{aligned}\tilde{L}_T^\kappa(1,\mp 1) &= \frac{1}{2Mc}\frac{1}{(2m_{\rm av}c^2)}\left\langle [R]_1 \left| \left[(\hat{\mathbf{i}}_x \pm i\hat{\mathbf{i}}_y)\cdot \hat{\boldsymbol{\pi}}_1 v_T^\kappa(r_{31}) \frac{z_{31}^2}{r_{31}^2} \right] \right| \phi_d(r_{21})\phi_d(r_{43}) \frac{F(r)}{\sqrt{R_0(\Delta R)^2}} Y_{1,\mp 1}(\theta,\phi) \right\rangle \\ &= \pm \text{Const} \int_0^\infty r^2 \mathrm{d}r \int \mathrm{d}^3\mathbf{r}_a \int \mathrm{d}^3\mathbf{r}_b\ \Phi_{4\rm He}(r, r_a, r_b, \theta_{ab})\phi_d(r_a)\phi_d(r_b) F(r) \\ &\quad \sqrt{\frac{8\pi}{3}} \left[\left(-\frac{2}{5}\frac{r^3}{r_{31}^4} - \frac{1}{2}\frac{r z_{ab}^2}{r_{31}^4} \right) + \left(\frac{1}{5}\frac{r^3}{r_{31}^3} + \frac{1}{4}\frac{r z_{ab}^2}{r_{31}^3} \right) \frac{\mathrm{d}}{\mathrm{d}r_{31}} \right] v_T^\kappa(r_{31}). \quad (158)\end{aligned}$$

These results (see Table 9) allow us to write

Table 9. Dimensionless spatial integrals for the tensor potential contribution to the interaction matrix element for $S = 1$, $M_S = 1$, $l = 1$ and $m = -1$; the matrix elements for the other case with $M_S = -1$ and $m = 1$ differ only by a sign.

Integral	eS	eT	oS	oT
$\tilde{I}_T^\kappa$	$i\ 1.17 \times 10^{-8}$	$i\ 9.42 \times 10^{-9}$	$i\ 1.17 \times 10^{-8}$	$i\ 6.01 \times 10^{-9}$
$\tilde{J}_T^\kappa$	$i\ 4.87 \times 10^{-9}$	$i\ 4.30 \times 10^{-9}$	$i\ 4.87 \times 10^{-9}$	$i\ 3.42 \times 10^{-9}$
$\tilde{K}_T^\kappa$	0	0	0	0
$\tilde{L}_T^\kappa$	$-i\ 3.75 \times 10^{-9}$	$-i\ 3.20 \times 10^{-9}$	$-i\ 3.75 \times 10^{-9}$	$-i\ 2.36 \times 10^{-9}$

$$M_T^{(S,M_S)} = \left[e^{-G\sqrt{\frac{R_0}{\langle R\rangle}\frac{(\Delta R)^2}{\langle(\Delta R)^2\rangle}}} \right]_{l=1} \times \begin{cases} -i(cP)\ 7.38 \times 10^{-8} & S=1,\ M_S=-1,\ l=1,\ m=\ 1 \\ 0 & S=1,\ M_S=\ 0,\ l=1,\ m=\ 0 \\ i(cP)\ 7.38 \times 10^{-8} & S=1,\ M_S=\ 1,\ l=1,\ m=-1 \end{cases} \tag{159}$$

10.3. Tensor potential contribution for $l = 3$

There is no contribution from the central potential interaction for the $l = 3$ case as discussed above. There is a contribution from the tensor potential, and we may write in this case

$$M_T^{(3,\pm1)} = (cP) \left[e^{-G\sqrt{\frac{R_0}{\langle R\rangle}\frac{(\Delta R)^2}{\langle(\Delta R)^2\rangle}}} \right]_{l=3} \sum_\kappa \tilde{A}_T^\kappa \tilde{I}_T^\kappa + \tilde{B}_T^\kappa \tilde{J}_T^\kappa + \tilde{C}_T^\kappa \tilde{K}_T^\kappa + \tilde{D}_T^\kappa \tilde{L}_T^\kappa, \tag{160}$$

The expansion coefficients are the same as above (see Table 7). The spatial integrals are

$$\tilde{I}_T^\kappa(1,\mp1) = \frac{1}{2Mc}\frac{1}{(2m_{\rm av}c^2)} \left\langle [R]_1 \left| \frac{z_{21}^2}{r_{21}^2} v_T^\kappa(r_{21}) \left[(\hat{\mathbf{i}}_x \pm \hat{\mathbf{i}}_y)\cdot\hat{\boldsymbol{\pi}}_1 \right] \right| \phi_d(r_{21})\phi_d(r_{43}) \frac{F(r)}{\sqrt{R_0(\Delta R)^2}} Y_{3,\mp1}(\theta,\phi) \right\rangle = 0, \tag{161}$$

$$\begin{aligned} \tilde{J}_T^\kappa(1,\mp1) &= \frac{1}{2Mc}\frac{1}{(2m_{\rm av}c^2)} \left\langle [R]_1 \left| \frac{z_{31}^2}{r_{31}^2} v_T^\kappa(r_{31}) \left[(\hat{\mathbf{i}}_x \pm \hat{\mathbf{i}}_y)\cdot\hat{\boldsymbol{\pi}}_1 \right] \right| \phi_d(r_{21})\phi_d(r_{43}) \frac{F(r)}{\sqrt{R_0(\Delta R)^2}} Y_{3,\mp1}(\theta,\phi) \right\rangle \\ &= \pm \text{Const} \int_0^\infty r^2 dr \int d^3\mathbf{r}_a \int d^3\mathbf{r}_b\ \Phi_{4\rm He}(r, r_a, r_b, \theta_{ab})\phi_d(r_a)\phi_d(r_b) v_T^\kappa(r_{31}) \\ &\quad \frac{8\sqrt{21\pi}}{105}\left(4\frac{r}{r_{31}^2} + \frac{r^2}{r_{31}^2}\frac{d}{dr} \right) F(r), \end{aligned} \tag{162}$$

$$\tilde{K}_T^\kappa(1,\mp1) = \frac{1}{2Mc}\frac{1}{(2m_{\rm av}c^2)} \left\langle [R]_1 \left| \left[(\hat{\mathbf{i}}_x \pm i\hat{\mathbf{i}}_y)\cdot\hat{\boldsymbol{\pi}}_1 v_T^\kappa(r_a) \frac{z_a^2}{r_a^2} \right] \right| \phi_d(r_a)\phi_d(r_b) \frac{F(r)}{\sqrt{R_0(\Delta R)^2}} Y_{3,\mp1}(\theta,\phi) \right\rangle = 0, \tag{163}$$

$$\tilde{L}_T^{\kappa}(1,\mp 1) = \frac{1}{2Mc}\frac{1}{(2m_{\rm av}c^2)}\left\langle [R]_1 \left| \left[(\hat{\mathbf{i}}_x \pm i\hat{\mathbf{i}}_y)\cdot\hat{\boldsymbol{\pi}}_1 v_T^{\kappa}(r_{31})\frac{z_{31}^2}{r_{31}^2}\right] \right| \phi_d(r_{21})\phi_d(r_{43})\frac{F(r)}{\sqrt{R_0(\Delta R)^2}}Y_{3,\mp 1}(\theta,\phi)\right\rangle$$
$$= \pm \text{Const}\int_0^{\infty} r^2 \mathrm{d}r \int \mathrm{d}^3\mathbf{r}_a \int \mathrm{d}^3\mathbf{r}_b\ \Phi_{4\rm He}(r,r_a,r_b,\theta_{ab})\phi_d(r_a)\phi_d(r_b)F(r)$$
$$\frac{8\sqrt{21\pi}}{105}\left(-\frac{r^3}{r_{31}^4} + \frac{r^3}{r_{31}^3}\frac{\mathrm{d}}{\mathrm{d}r_{31}}\right) v_T^{\kappa}(r_{31}). \tag{164}$$

Numerical results are presented in Table 10. We can use these results to write

$$M_T^{(S,M_S)} = \left[\mathrm{e}^{-G\sqrt{\frac{R_0}{\langle R\rangle}\frac{(\Delta R)^2}{\langle(\Delta R)^2\rangle}}}\right]_{l=3}$$
$$\times \begin{cases} i(cP)\ 1.45\times 10^{-9} & S=1,\ M_S=-1,\ l=3,\ m=\ 1 \\ 0 & S=1,\ M_S=\ 0,\ l=3,\ m=\ 0 \\ -i(cP)\ 1.45\times 10^{-9} & S=1,\ M_S=\ 1,\ l=3,\ m=-1 \end{cases} \tag{165}$$

11. Summary and discussion

We have computed central and tensor interaction contributions to the phonon exchange matrix elements for $D_2/^4$He transitions based on the new $\mathbf{a}\cdot c\mathbf{P}$ coupling between vibrations and internal nuclear degrees of freedom described in [12], using simplified nuclear models in connection with the Hamada–Johnston nucleon–nucleon potential. We find nonzero coupling to the molecular ^{3}P and ^{3}F states, with the largest interaction in the case of ^{3}P; the interaction Hamiltonian for both the central and tensor interactions together in this model for z-directed motion and/or vector potential is

$$\hat{H}_{\rm int} = i\ 5.03\times 10^{-8}\left(c\hat{P}_z - Ze\hat{A}_z\right)\left[\mathrm{e}^{-G\sqrt{\frac{R_0}{\langle R\rangle}\frac{(\Delta R)^2}{\langle(\Delta R)^2\rangle}}}\right]_{l=1}$$
$$\left\{ \left|\Psi[^4\text{He}]\right\rangle\left\langle\Psi[\text{D}_2\ ^3\text{P}(M_S=1,m=-1)]\right| - \left|\Psi[^4\text{He}]\right\rangle\left\langle\Psi[\text{D}_2\ ^3\text{P}(M_S=-1,m=1)]\right|\right\} + \text{Hc.}, \tag{166}$$

where "Hc." indicates the Hermitian conjugate, for z-directed vibrations. We have augmented the center of mass momentum from the text with the vector potential following the discussion of Section 5. The coupling in the case of the molecular ^{3}F states is more

Table 10. Dimensionless spatial integrals for the tensor potential contribution to the interaction matrix element for $S=1$, $M_S=1$, $l=3$ and $m=-1$; the matrix elements for the other case with $M_S=-1$ and $m=1$ differ only by a sign.

Integral	eS	eT	oS	oT
$\tilde{I}_T^{\kappa}$	0	0	0	0
$\tilde{J}_T^{\kappa}$	$i\ 3.08\times 10^{-9}$	$i\ 2.73\times 10^{-9}$	$i\ 3.08\times 10^{-9}$	$i\ 2.19\times 10^{-9}$
$\tilde{K}_T^{\kappa}$	0	0	0	0
$\tilde{L}_T^{\kappa}$	$-i\ 1.90\times 10^{-9}$	$-i\ 1.61\times 10^{-9}$	$-i\ 1.90\times 10^{-9}$	$-i\ 1.61\times 10^{-9}$

than two orders of magnitude smaller, and there is no coupling to the singlet and quintet molecular states due to central and tensor contributions. The phase factor i that appears is due to the definition of the triplet molecular relative wavefunction as real; other conventions are possible, and subsequent calculations that might involve this interaction potential are not impacted by this phase convention.

It is possible to understand this result in connection with a relative volume argument that we have used previously [22]. Not only do the two deuterons need to tunnel through the Coulomb barrier in order to interact, but they also need to localize from the molecular scale to the nuclear scale. As a result, we can think of the interaction Hamiltonian for a specific transition as

$$\hat{H}_{\rm int} \;=\; \left[{\rm e}^{-G} \sqrt{\frac{v_{\rm nuc}}{v_{\rm mol}}} \right]_{l=1} \; (c\hat{P}_z - ZeA_z)\; i\; (\cdots), \tag{167}$$

where $v_{\rm mol}$ is the characteristic molecular volume, where $v_{\rm nuc}$ is a characteristic nuclear volume, and where $(\cdots)$ is the interaction strength for deuterons localized on a nuclear scale. If we take for the ratio

$$\frac{v_{\rm nuc}}{v_{\rm mol}} \;=\; \frac{\frac{4}{3}\pi r_{\rm nuc}^3}{2\pi^2 R_0 \Delta R^2} \;=\; 6.26 \times 10^{-12} \tag{168}$$

using $r_{\rm nuc} = 5$ fm, then we can estimate

$$|(\cdots)| \;=\; 0.020. \tag{169}$$

Since the $\hat{\mathbf{a}}$ operator of the $\mathbf{a} \cdot (c\mathbf{P})$ interaction is a velocity operator normalized to the speed of light [11], the associated transition matrix element (which has magnitude $|(\cdots)|$) can be no larger than unity. The magnitude of the transition matrix element in the case of coupling to the deuteron was estimated to be about $0.003(cP)$. We might have expected a volume corrected interaction matrix element calculated in this paper to have a similar magnitude (of 0.003); however, the result that we obtained is somewhat larger (due primarily to the effect of the relative deuteron–deuteron potential). Our basic conclusion at this point is that the magnitude of the interaction Hamiltonian calculated in this paper seems to us to be reasonable given the previous calculation for the deuteron transition.

We have focused in this work on the central and tensor contributions to the interaction, since these are the strongest. Our attention might reasonably have been focused on the spin–orbit contribution, which would produce different selection rules (including singlet and quintet coupling, with allowed coupling to the $l = 0$ rotational state). Such a project is of interest, but there are complications. The $\mathbf{a} \cdot c\mathbf{P}$ coupling that we are interested in is closely related to spin–orbit coupling, so it will be necessary to examine the derivation of the new interaction specifically for the spin–orbit interaction (which would involve going to higher order than was done in [11]). In the case of the Hamada–Johnston model, the spin–orbit coupling model is not derived as a normal spin–orbit coupling based on the central and tensor interactions, but is itself independent and empirical. As such, one wonders whether such a model is appropriate for an $\mathbf{a} \cdot c\mathbf{P}$ interaction. Nevertheless we have carried out some exploratory computations for the spin–orbit contribution for the singlet $l = 0$ case, and the relevant spatial integrals appear to be much smaller than for the central and tensor cases.

The advantage of using simplified wavefunctions and the Hamada–Johnston potential in the calculations presented in this paper is primarily that we are able to carry out a reasonable first pass at the largest contribution to the interaction matrix element without too much effort. It is certainly possible to do a better job, and it seems worthwhile to comment on some of the issues that seem important in the calculation. First and foremost seems to be the deuteron–deuteron interaction potential, since the magnitude of the probability amplitude at the fermi scale is very sensitive to this potential (for our calculation we have relied on empirical Woods–Saxon potentials optimized to match experimental phase shifts). The use of simplified ^{4}He and deuteron wavefunctions with no D-state admixture is expected to produce errors in the matrix element perhaps at the 50% level, based on our experience with the coupling matrix element calculation for the deuteron. The simplicity of the assumed product wavefunctions for both the initial and final states will lead to errors. In addition we expect errors associated with the use of the Hamada–Johnston potential (although these are likely small compared to those already mentioned).

It is possible to do a better job in all areas. For example, impressive results have been obtained in recent years with nuclear calculations based on chiral effective field theory [23]. There are by now many modern calculations of ^{4}He, such as described in [24–26]. There is a growing literature that make use of modern potentials and methods for four-nucleon scattering and reaction

calculations. Groups that work in this area would have little difficulty in applying their models to the calculation of the phonon exchange transition matrix element done more simply in this work.

Appendix A. Hamada–Johnston potential

The Hamada–Johnston potential can be written as [15]

$$\hat{V} \;=\; (\boldsymbol{\sigma}_1\cdot\boldsymbol{\sigma}_2)(\boldsymbol{\tau}_1\cdot\boldsymbol{\tau}_2)v_C(r)+(\boldsymbol{\tau}_1\cdot\boldsymbol{\tau}_2)\hat{S}_{12}v_T(r)+\left(\frac{\hat{\mathbf{L}}\cdot\hat{\mathbf{S}}}{\hbar^2}\right)v_{LS}(r)+\left(\frac{\hat{L}_{12}}{\hbar^2}\right)v_{LL}(r). \tag{A.1}$$

Appendix A.1. Central potential

The first term is the central potential with

$$v_C(r) \;=\; 0.08\frac{m_\pi c^2}{3}Y(\alpha r)\Big[1+a_C Y(\alpha r)+b_C Y^2(\alpha r)\Big], \tag{A.2}$$

where $Y(x)$ is defined according to

$$Y(x) \;=\; \frac{\mathrm{e}^{-x}}{x}. \tag{A.3}$$

Appendix A.2. Tensor interaction

The second term is the tensor interaction where

$$v_T(r) \;=\; 0.08\frac{m_\pi c^2}{3}Z(\alpha r)\Big[1+a_T Y(\alpha r)+b_T Y^2(\alpha r)\Big], \tag{A.4}$$

$$\hat{S}_{12} \;=\; 3\frac{(\boldsymbol{\sigma}_1\cdot\mathbf{r})(\boldsymbol{\sigma}_2\cdot\mathbf{r})}{r^2}-(\boldsymbol{\sigma}_1\cdot\boldsymbol{\sigma}_2). \tag{A.5}$$

Appendix A.3. Spin–orbit interaction

The third term is the spin–orbit interaction

$$v_{LS}(r) \;=\; G_{LS}m_\pi c^2 Y^2(\alpha r)\big[1+b_{LS}Y(\alpha r)\big], \tag{A.6}$$

$$\hat{\mathbf{L}} \;=\; (\mathbf{r}_2-\mathbf{r}_1)\times(\mathbf{p}_2-\mathbf{p}_1), \tag{A.7}$$

$$\hat{\mathbf{S}} \;=\; \frac{\hbar}{2}(\boldsymbol{\sigma}_1+\boldsymbol{\sigma}_2). \tag{A.8}$$

Appendix A.4. Quadratic spin–orbit interaction

The last term is a quadratic spin–orbit term with

$$v_{LL}(r) \;=\; G_{LL}m_\pi c^2\frac{Z(\alpha r)}{(\alpha r)^2}\Big[1+a_{LL}Y(\alpha r)+b_{LL}Y^2(\alpha r)\Big], \tag{A.9}$$

$$\hat{L}_{12} \;=\; (\boldsymbol{\sigma}_1\cdot\boldsymbol{\sigma}_2)|\hat{\mathbf{L}}|^2-\frac{1}{2}(\boldsymbol{\sigma}_1\cdot\hat{\mathbf{L}})(\boldsymbol{\sigma}_2\cdot\hat{\mathbf{L}})-\frac{1}{2}(\boldsymbol{\sigma}_2\cdot\hat{\mathbf{L}})(\boldsymbol{\sigma}_1\cdot\hat{\mathbf{L}}). \tag{A.10}$$

The Z function is defined according to

$$Z(x) \;=\; Y(x)\left(1+\frac{3}{x}+\frac{3}{x^2}\right). \tag{A.11}$$

Appendix A.5. Parametrization

The various a and b parameters are channel-dependent fitting coefficients which have been tabulated in [15]. The α parameter in the Hamada–Johnston potential is taken to satisfy

$$\frac{1}{\alpha} \;=\; 1.415 \text{ fm}. \tag{A.12}$$

The pion mass is taken to be

$$m_\pi c^2 \;=\; 139.4 \text{ MeV}. \tag{A.13}$$

The Hamada–Johnston potential is a hard core potential, so the potential is assumed to be infinitely repulsive at small relative position

$$v_{12} \;=\; \infty, \qquad \alpha r < 0.343. \tag{A.14}$$

Appendix A.6. Projection operators

The different potentials in the Hamada–Johnston model depend on whether the spin of the two interacting nucleons is singlet or triple, and whether the relative spatial wavefunction is even or odd. To implement this one can make use of spin and isospin projection operators, by taking advantage of antisymmetry. We know that the wavefunction for two nucleons must be antisymmetric if the two nucleons are exchanged, and that this antisymmetry is reflected in the spatial, spin and isospin components of the wavefunction. So, if the relative spatial wavefunction is even (symmetric), and the nucleon spins are in a triplet configuration (also symmetric), then the isospin wavefunction must be singlet (antisymmetric). We can use this to write

$$\hat{v}_C(r) \;=\; v_C^{eS}(r)\hat{P}_S^{(a)}\hat{P}_T^{(s)} + v_C^{eT}(r)\hat{P}_S^{(s)}\hat{P}_T^{(a)} + v_C^{oS}(r)\hat{P}_S^{(a)}\hat{P}_T^{(a)} + v_C^{oT}(r)\hat{P}_S^{(s)}\hat{P}_T^{(s)}, \tag{A.15}$$

where the $\hat{P}$ operators are projection operators

$$\hat{P}_S^{(a)}(12) \;=\; -\frac{1}{4}\Big[\boldsymbol{\sigma}_1\cdot\boldsymbol{\sigma}_2 - I\Big] \qquad \hat{P}_S^{(s)}(12) \;=\; \frac{1}{4}\Big[\boldsymbol{\sigma}_1\cdot\boldsymbol{\sigma}_2 + 3I\Big], \tag{A.16}$$

$$\hat{P}_T^{(a)}(12) \;=\; -\frac{1}{4}\Big[\tau_1\cdot\boldsymbol{\tau}_2 - I\Big] \qquad \hat{P}_T^{(s)}(12) \;=\; \frac{1}{4}\Big[\boldsymbol{\tau}_1\cdot\boldsymbol{\tau}_2 + 3I\Big]. \tag{A.17}$$

References

[1] P.L. Hagelstein, Bird's eye view of phonon models for excess heat in the Fleischmann—Pons experiment, *J. Condensed Matter Nucl. Sci.* **6** (2011) 169.
[2] M. Fleischmann, S. Pons and M. Hawkins, *J. Electroanal Chem.* **201** (1989) 301; errata, **263** (1990) 187.
[3] M. Fleischmann, S. Pons, M.W. Anderson, L.J. Li and M. Hawkins, *J. Electroanal. Chem.* **287** (1990) 293.
[4] P.L. Hagelstein, M.C.H. McKubre, D.J. Nagel, T.A. Chubb and R.J. Hekman, *Proc. ICCF11*, 2004, p. 23.
[5] P.L. Hagelstein, *Naturwissenschaften* **97** (2010) 345.
[6] P.L. Hagelstein and I.U. Chaudhary, Energy exchange in the lossy spin-boson model, *J. Condensed Matter Nucl. Sci.* **5** (2011) 52.

[7] P.L. Hagelstein and I.U. Chaudhary, Second-order formulation and scaling in the lossy spin-boson model, *J. Condensed Matter Nucl. Sci.* **5** (2011) 87.
[8] P.L. Hagelstein and I.U. Chaudhary, Local approximation for the lossy spin—boson model, *J. Condensed Matter Nucl. Sci.* **5** (2011) 102.
[9] P.L. Hagelstein and I.U. Chaudhary, Coherent energy exchange in the strong coupling limit of the lossy spin-boson model, *J. Condensed Matter Nucl. Sci.* **5** (2011) 116.
[10] P.L. Hagelstein and I.U. Chaudhary, Generalization of the lossy spin—boson model to donor and receiver systems, *J. Condensed Matter Nucl. Sci.* **5** (2011) 140.
[11] P.L. Hagelstein and I.U. Chaudhary, Including nuclear degrees of freedom in a lattice Hamiltonian, *J. Condensed Matter Nucl. Sci.* **7** (2011) 35.
[12] P.L. Hagelstein and I.U. Chaudhary, Coupling between a deuteron and a lattice, *J. Condensed Matter Nucl. Sci.* **9** (2012) 50.
[13] F.J. Wilkinson III and F.J. Cecil, *Phys. Rev. C* **31** (1985) 2036.
[14] H.J. Assenbaum and K. Langanke, *Phys. Rev. C* **36** (1987) 17.
[15] H.J. Boersma, *Nucl. Phys.* **A135** (1969) 609.
[16] T. Hamada and I.D. Johnston, A potential model representation of two-nucleon data below 315 MeV, *Nucl. Phys.* **34** (1962) 382.
[17] I.U. Chaudhary, *Applications of Group Theory to Few-Body Physics*, MIT PhD Thesis (2005).
[18] I.U. Chaudhary and P.L. Hagelstein, Four-body RST general nuclear wavefunctions and matrix elements, *Proc. ICCF12* (2005) 527.
[19] J. Carlson, *Phys. Rev. C* **38** (1988) 1879.
[20] E.L. Tomusiak, W. Leidemann and H.M. Hofmann, *Phys. Rev. C* **52** (1995) 1963.
[21] A.A. Frost and B. Musulin, *J. Chem. Phys.* **22** (1954) 1017.
[22] P.L. Hagelstein, Phonon exchange models: Some new results, *Proc. ICCF11*, 2004, p. 743.
[23] R. Machleidt and D.R. Entem, Chiral effective field theory and nuclear forces, *Physics Reports* **503** (2011) 1.
[24] H. Kamada, A. Nogga, W.Glöckle, E. Hiyama, M. Kamimura, K. Varga, Y. Suzuki, M. Viviani, A. Kievsky, and S. Rosati, Benchmark test calculation of a four-nucleon bound state, *Phys. Rev. C* **64** (2001) 044001.
[25] L. Coraggio, A. Covello, A. Gargano, N. Itaco, T.T.S. Kuo and R. Machleidt, *Phys. Rev. C* **271** (2005) 014307-1.
[26] J. Kirscher, H.W. Griesshammer, D. Shukla and H.M. Hofmann, *Eur. Phys. J. A* **44** (2010) 239.